

## BOLD and EEG Signal Variability at Rest Differently Relate to Aging in the Human Brain

D. Kumral<sup>1,2</sup>, F. Şansal<sup>3,1</sup>, E. Cesnaite<sup>1</sup>, K. Mahjoory<sup>1,4</sup>, E. Al<sup>2,1</sup>, M. Gaebler<sup>1,2</sup>, V. V. Nikulin<sup>1,5,6</sup>, A. Villringer<sup>1,2,7,8</sup>

<sup>1</sup>Department of Neurology, Max Planck Institute for Human Cognitive and Brain Sciences, Leipzig, Germany

<sup>2</sup>MindBrainBody Institute at the Berlin School of Mind and Brain, Humboldt-Universität zu Berlin, Berlin, Germany

<sup>3</sup>International Graduate Program Medical Neurosciences, Charité-Universitätsmedizin, Berlin, Germany

<sup>4</sup>Institute for Biomagnetism and Biosignalanalysis, University of Muenster, Muenster, Germany

<sup>5</sup>Neurophysics Group, Department of Neurology, Campus Benjamin Franklin, Charité Universitätsmedizin Berlin, Berlin, Germany

<sup>6</sup>Centre for Cognition and Decision Making, National Research University Higher School of Economics, Moscow, Russian Federation

<sup>7</sup>Center for Stroke Research Berlin, Charité – Universitätsmedizin Berlin, Berlin, Germany

<sup>8</sup>Department of Cognitive Neurology, University Hospital Leipzig

**Corresponding author:** Deniz Kumral, Department of Neurology, Max Planck Institute for Human Cognitive and Brain Sciences, Stephanstrasse 1A, 04103, Leipzig, Germany.  
Email: [dkumral@cbs.mpg.de](mailto:dkumral@cbs.mpg.de)

**Abbreviations:** BOLD – Blood Oxygenation Level Dependent; CBF – cerebral blood flow; CBV – cerebral blood volume; CCA – canonical correlation analysis; CMRO<sub>2</sub> – cerebral metabolic rate of oxygen; CVR – cerebrovascular reactivity; DMN – Default Mode Network; EEG – electroencephalography; EC – eyes closed; EO – eyes open; framewise displacement – FD; FDR - false discovery rate; FEM – finite element method; fMRI – functional Magnetic Resonance Imaging; fNIRS – functional Near-Infrared Spectroscopy; FWHM – full-width half-maximum; ICBM – International Consortium for Brain Mapping; MEG – magnetoencephalography; MNI – Montreal Neurological Institute; rho – Spearman’s rank correlation coefficient; PET –Positron-emission tomography; ROI – regions of interests; rs – resting state; SD – standard deviation; SVD – Singular Value Decomposition; TIV–Total Intracranial Volume

1

## Abstract

2 Variability of neural activity is regarded as a crucial feature of healthy brain function, and  
3 several neuroimaging approaches have been employed to assess it noninvasively. Studies on  
4 the variability of both evoked brain response and spontaneous brain signals have shown  
5 remarkable changes with aging but it is unclear if the different measures of brain signal  
6 variability – identified with either hemodynamic or electrophysiological methods – reflect the  
7 same underlying physiology. In this study, we aimed to explore age differences of  
8 spontaneous brain signal variability with two different imaging modalities (EEG, fMRI) in  
9 healthy younger ( $25 \pm 3$  years,  $N=135$ ) and older ( $67 \pm 4$  years,  $N=54$ ) adults. Consistent with  
10 the previous studies, we found lower blood oxygenation level dependent (BOLD) variability  
11 in the older subjects as well as less signal variability in the amplitude of low-frequency  
12 oscillations (1–12 Hz), measured in source space. These age-related reductions were mostly  
13 observed in the areas that overlap with the default mode network. Moreover, age-related  
14 increases of variability in the amplitude of beta-band frequency EEG oscillations (15–25 Hz)  
15 were seen predominantly in temporal brain regions. There were significant sex differences in  
16 EEG signal variability in various brain regions while no significant sex differences were  
17 observed in BOLD signal variability. Bivariate and multivariate correlation analyses revealed  
18 no significant associations between EEG- and fMRI-based variability measures. In summary,  
19 we show that both BOLD and EEG signal variability reflect aging-related processes but are  
20 likely to be dominated by different physiological origins, which relate differentially to age  
21 and sex.

22 **Keywords:** brain signal variability, resting state, BOLD, fMRI, EEG, aging, sex, default  
23 mode network

24

## 1. Introduction

25 Functional neuroimaging methods such as fMRI, PET, fNIRS, EEG, or MEG have  
26 allowed the non-invasive assessment of functional changes in the aging human brain (Cabeza,  
27 2001; Cabeza et al., 2018). Most previous functional neuroimaging studies on aging have  
28 employed a task-based design (Grady, 2012) and in their data analysis the central tendency  
29 has typically been assumed to be the most representative value in a distribution (e.g., mean)  
30 (Speelman and McGann, 2013) or the “signal” within distributional “noise”. In recent years,  
31 also the variability of brain activation in task-dependent and task-independent measurements  
32 (as spontaneous variations of background activity) has been shown to provide relevant  
33 information about the brain’s functional state (Garrett et al., 2013b; Grady and Garrett, 2018;  
34 Nomi et al., 2017). These studies primarily measured the blood oxygen level dependent  
35 (BOLD) signal using fMRI. For example, it has been demonstrated that the variance of the  
36 task-evoked BOLD response was differentially related to aging as well as cognitive  
37 performance (Armbruster-Genc et al., 2016; Garrett et al., 2013a). Similarly, spontaneous  
38 signal variability in resting state fMRI (rsfMRI) has been found to decrease with age (Grady  
39 and Garrett, 2018; Nomi et al., 2017), in individuals with stroke (Kielar et al., 2016), and  
40 22q11.2 deletion syndrome (Zöller et al., 2017). An increase of fMRI variability has been  
41 shown to occur in inflammation induced state-anxiety (Labrenz et al., 2018) and to parallel  
42 symptom severity in Attention Deficit Hyperactivity Disorder (Nomi et al., 2018). From these  
43 studies, it was concluded that changes in BOLD signal variability might serve as an index for  
44 alterations in neural processing and cognitive flexibility (Grady and Garrett, 2014).

45 The conclusions of aforementioned studies imply that BOLD signal variability is  
46 mainly determined by *neuronal* variability. To a large extent, this is based on the premise that  
47 BOLD is related to neuronal activity: The evoked BOLD signal in task-based fMRI reflects  
48 the decrease of the deoxyhemoglobin concentration to changes in local brain activity, which is  
49 determined by vascular (blood velocity and volume: “neurovascular coupling”) and metabolic  
50 (oxygen consumption: “neurometabolic coupling”) factors (Logothetis and Wandell, 2004;  
51 Villringer and Dirnagl, 1995). The BOLD signal is therefore only an indirect measure of  
52 neural activity (Logothetis, 2008). For the variability of task-evoked BOLD signal and for  
53 spontaneous variations of the BOLD signal, in principle, the same considerations apply  
54 regarding their relationship to underlying neural processes (Murayama et al., 2010). However,  
55 since in rsfMRI there is no explicit external trigger for evoked brain activity to which time-  
56 locked averaging could be applied, the time course of rsfMRI signals is potentially more  
57 susceptible to contributions of “physiological noise”, such as cardiac and respiratory signals

58 (Birn et al., 2008; Chang et al., 2009), but also spontaneous fluctuations of vascular tone,  
59 which is found even in isolated arterial vessels (Failla et al., 1999; Hudetz et al., 1998; Wang  
60 et al., 2006). In the same vein, the variability of task-evoked fMRI is not necessarily  
61 reflecting only the variability of evoked neuronal activity, as it may also – at least partly –  
62 reflect the variability of the spontaneous background signal on which a constant evoked  
63 response is superimposed.

64 In aging, non-neuronal signal fluctuations may also introduce spurious common  
65 variance across the rsfMRI time series (Caballero-Gaudes and Reynolds, 2017), thus  
66 confounding estimates of “neural” brain signal variability. Previous evidence suggests that the  
67 relationship between neuronal activity and the vascular response is attenuated with age – and  
68 so is, as a consequence, the BOLD signal (for review see D’Esposito et al., 2003). For  
69 instance, aging has been associated with altered cerebrovascular ultrastructure, reduced  
70 elasticity of vessels, and atherosclerosis (Farkas and Luiten, 2001) but also with a decrease in  
71 resting cerebral blood flow (CBF), cerebral metabolic rate of oxygen (CMRO<sub>2</sub>), and  
72 cerebrovascular reactivity (CVR) (Liu et al., 2013). Taken together, age-related changes in  
73 BOLD signal or BOLD signal variability are related to a mixture of alterations in non-neuronal  
74 spontaneous fluctuations of vascular signals, neural activity, neurovascular coupling, and/or  
75 neurometabolic coupling (D’Esposito et al., 2003; Geerligs et al., 2017; Tsvetanov et al.,  
76 2015).

77 While BOLD fMRI signal and specifically variance measures based on fMRI are only  
78 partially and indirectly related to neural activity (Liu, 2013; Logothetis, 2008),  
79 electrophysiological methods such as EEG can provide a more direct assessment of neural  
80 activity with a higher temporal but poorer spatial resolution (Cohen, 2017). EEG measures  
81 neuronal currents resulting from the synchronization of dendritic postsynaptic potentials  
82 across the neural population; the cerebral EEG rhythms thereby reflect the underlying brain  
83 neural network activity (Steriade, 2006). Resting state (rs)EEG is characterized by  
84 spontaneous oscillations (“brain rhythms”) at different frequencies. Previously, the mean  
85 amplitude of low-frequency bands (e.g., delta and/or theta, 1-7 Hz) has been shown to  
86 correlate negatively with age (Vlahou et al., 2015), while higher-frequency bands (e.g., beta,  
87 15-25 Hz) show the reverse pattern (Rossiter et al., 2014). However, less is known about the  
88 within-subject variability of EEG measures and their association with aging. Several studies  
89 have addressed the variability in the spectral amplitudes of different frequency bands using  
90 variance (Hawkes and Prescott, 1973; Oken and Chiappa, 1988), coefficient of variation  
91 (Burgess and Gruzelier, 1993; Maltez et al., 2004), and complexity (Fernández et al., 2012;

92 Sleimen-Malkoun et al., 2015). For instance, reductions of the complexity in rsEEG signal  
93 have been found not only in healthy aging (Yang et al., 2013; Zappasodi et al., 2015) but also  
94 in age-related pathologies such as mild cognitive impairment (McBride et al., 2014) and  
95 Alzheimer's disease (Smits et al., 2016). Accordingly, it has been suggested that irregular  
96 (e.g., variable) systems indicate a normal and healthy state (more integrated information)  
97 while highly regular systems often mark dysfunction or disease (Lipsitz and Goldberger,  
98 1992; Vaillancourt and Newell, 2002).

99 The different methodological approaches, fMRI based “vascular” approaches on the  
100 one hand and electrophysiological methods such as EEG and MEG, on the other hand,  
101 indicate alterations of brain signal variability with aging. However, it remains unclear whether  
102 these different measures of brain variability at rest reflect the same underlying physiological  
103 changes. Evidently, there are some correlations between the two signal sources (for a review  
104 see, Jorge et al., 2014; Ritter and Villringer, 2006). For instance, in task-based EEG-fMRI  
105 simultaneous recordings, a relationship between BOLD responses and amplitude of evoked  
106 potentials has been demonstrated (e.g., Ritter et al., 2009; Seaquist et al., 2007), while in  
107 resting state EEG-fMRI studies, a negative association between spontaneous modulations of  
108 alpha rhythm and BOLD signal has also been established (e.g., Chang et al., 2013; Goldman  
109 et al., 2002; Gonçalves et al., 2006; Moosmann et al., 2003). Further, differential correlation  
110 patterns have been noted for the various rhythms of different frequencies in EEG/MEG and  
111 the fMRI signal, such that low-frequency oscillations show a negative (Deligianni et al., 2014;  
112 Mantini et al., 2007; Meyer et al., 2013), while higher frequencies oscillations demonstrate a  
113 positive correlation with the BOLD signal (Niessing et al., 2005; Scheeringa et al., 2011).

114 Regarding the known age-related changes in BOLD and EEG signal variability,  
115 respectively, the question arises whether these alterations are dominated by joint signal  
116 sources of fMRI and EEG or by – potentially different – signal contributions that relate to  
117 each of these two methods. Given the – potentially large – non-neuronal signal contribution,  
118 this issue is particularly relevant for rsfMRI studies. Here, we addressed this question by  
119 analyzing rsfMRI and EEG measures of variability in healthy younger and older subjects. To  
120 our knowledge, the only study that compared variability in a “vascular” imaging method  
121 (rsfMRI) and an electrophysiological method (rsMEG at the sensor space) concluded that the  
122 effects of aging on BOLD signal variability were mainly driven by vascular factors (e.g.,  
123 heart rate variability) and not well-explained by the changes in neural variability (Tsvetanov  
124 et al., 2015). The main aims of the present study were to explore i) age differences of brain  
125 signal variability measures, as well as to investigate ii) how neural variability derived from

126 rsEEG related to the analogous parameters of BOLD signal variability derived from rsfMRI.  
127 We used rsfMRI and rsEEG from the “Leipzig Study for Mind-Body-Emotion Interactions”  
128 (Babayan et al., 2019). As an explanatory analysis, we further investigated sex-related  
129 differences of brain signal variability measures. To measure brain signal variability, we  
130 calculated the standard deviation (SD) of both the BOLD signal and of the amplitude  
131 envelope of the filtered rsEEG time series for a number of standard frequency bands at the  
132 source space. We hypothesized that brain signal variability would generally decrease with  
133 aging. In addition, based on the premise that BOLD fMRI signal variability reflects *neural*  
134 variability as measured by rsEEG, we expected that the corresponding changes in both signal  
135 modalities would demonstrate moderate to strong similarity in their spatial distribution. Given  
136 the confounding effects of vascular factors during aging on the fMRI signal (D’Esposito et al.,  
137 2003; Liu, 2013; Thompson, 2018), we further expected to find the relationship between  
138 BOLD and EEG signal variability to be stronger in younger than older adults.

139

## 2. Method

140

### 2.1. Participants

141

The data of the “Leipzig Study for Mind-Body-Emotion Interactions” (LEMON;

142

Babayan et al., 2019) comprised 227 subjects in two age groups (younger: 20-35, older: 59-

143

77). Only participants who did not report any neurological disorders, head injury, alcohol or

144

other substance abuse, hypertension, pregnancy, claustrophobia, chemotherapy and malignant

145

diseases, current and/or previous psychiatric disease or any medication affecting the

146

cardiovascular and/or central nervous system in a telephone pre-screening were invited to the

147

laboratory. The study protocol conformed to the Declaration of Helsinki and was approved by

148

the ethics committee at the medical faculty of the University of Leipzig (reference number

149

154/13-ff).

150

RsEEG recordings were available for 216 subjects who completed the full study

151

protocol. We excluded data from subjects that had missing event information (N=1), different

152

sampling rate (N=3), mismatching header files or insufficient data quality (N=9). Based on

153

the rsfMRI quality assessment, we further excluded data from subjects with faulty

154

preprocessing (N=7), ghost artefacts (N=2), incomplete data (N=1), or excessive head motion

155

(N=3) (criterion: mean framewise displacement (FD)  $\leq 0.5$  mm; Power et al., 2012)

156

(Supplementary Figure 1). The final sample included 135 younger ( $M = 25.10 \pm 3.70$  years,

157

42 females) and 54 older subjects ( $M = 67.15 \pm 4.52$  years, 27 females).

158

### 2.1. fMRI Acquisition

159

Brain imaging was performed on a 3T Siemens Magnetom Verio MR scanner

160

(Siemens Medical Systems, Erlangen, Germany) with a standard 32-channel head coil. The

161

participants were instructed to keep their eyes open and not fall asleep while looking at a low-

162

contrast (light grey on dark grey background) fixation cross.

163

The structural image was recorded using an MP2RAGE sequence (Marques et al., 2010) with

164

the following parameters: TI 1 = 700 ms, TI 2 = 2500 ms, TR = 5000 ms, TE = 2.92 ms, FA 1

165

= 4°, FA 2 = 5°, band width = 240 Hz/pixel, FOV = 256  $\times$  240  $\times$  176 mm<sup>3</sup>, voxel size = 1 x 1

166

x 1 mm<sup>3</sup>. The functional images were acquired using a T2\*-weighted multiband EPI sequence

167

with the following parameters: TR = 1400 ms, TE = 30 ms, FA = 69°, FOV = 202 mm,

168

imaging matrix = 88  $\times$  88, 64 slices with voxel size = 2.3 x 2.3 x 2.3 mm<sup>3</sup>, slice thickness = 2.3

169

mm, echo spacing = 0.67 ms, bandwidth = 1776 Hz/Px, partial fourier 7/8, no pre-scan

170

normalization, multiband acceleration factor = 4, 657 volumes, duration = 15 min 30 s. A

171

gradient echo field map with the sample geometry was used for distortion correction (TR =

172

680 ms, TE 1 = 5.19 ms, TE 2 = 7.65 ms).

173

## 2.2.fMRI Preprocessing

174

Preprocessing was implemented in Nipype (Gorgolewski et al., 2011), incorporating tools from FreeSurfer (Fischl, 2012), FSL (Jenkinson et al., 2012), AFNI (Cox, 1996), ANTs (Avants et al., 2011), CBS Tools (Bazin et al., 2014), and Nitime (Rokem et al., 2009). The pipeline comprised the following steps: (I) discarding the first five EPI volumes to allow for signal equilibration and steady state, (II) 3D motion correction (FSL mcflirt), (III) distortion correction (FSL fugue), (IV) rigid body coregistration of functional scans to the individual T1-weighted image (Freesurfer bbregister), (V) denoising including removal of 24 motion parameters (CPAC, Friston et al., 1996), motion, signal intensity spikes (Nipype rapidart), physiological noise in white matter and cerebrospinal fluid (CSF) (CompCor; Behzadi et al., 2007), together with linear and quadratic signal trends, (VI) band-pass filtering between 0.01-0.1 Hz (FSL fslmaths), (VII) spatial normalization to MNI152 (Montreal Neurological Institute) standard space (2 mm isotropic) via transformation parameters derived during structural preprocessing (ANTs). (VIII) The data were then spatially smoothed with a 6-mm full-width half-maximum (FWHM) Gaussian kernel (FSL fslmaths). Additionally, we calculated total intracranial volume (TIV) of each subject using the Computational Anatomy Toolbox (CAT12: <http://dbm.neuro.uni-jena.de/cat/>) running on Matlab 9.3 (Mathworks, Natick, MA, USA) and used it as a covariate for further statistical analyses (Malone et al., 2015).

192

*BOLD Signal Variability (SD<sub>BOLD</sub>)*. Standard deviation (SD) quantifies the amount of variation or dispersion in a set of values (Garrett et al., 2015; Grady and Garrett, 2018). Higher SD in rsfMRI signal indicates greater intensity of signal fluctuation or an increased level of activation in a given area (Garrett et al., 2011). We first calculated SD<sub>BOLD</sub> across the whole time series for each voxel and then within 96 boundaries of preselected atlas-based regions of interests (ROIs) based on the Harvard-Oxford cortical atlas (Desikan et al., 2006). The main steps of deriving brain signal variability (SD<sub>BOLD</sub>) from the preprocessed fMRI signal are shown in Figure 1.

200

The reproducible workflows containing fMRI preprocessing details can be found here:

<https://github.com/NeuroanatomyAndConnectivity/pipelines/releases/tag/v2.0>.

202

## 2.3.EEG Recordings

203

Sixteen minutes of rsEEG were acquired on a separate day with BrainAmp MR-plus amplifiers using 61 ActiCAP electrodes (both Brain Products, Germany) attached according to the international standard 10-20 localization system (Jurcak et al., 2007) with FCz (fronto-central or cephalic electrode) as the reference. The ground electrode was located at the

207 sternum. Electrode impedance was kept below 5 k $\Omega$ . Continuous EEG activity was digitized  
208 at a sampling rate of 2500 Hz and band-pass filtered online between 0.015 Hz and 1 kHz.

209 The experimental session was divided into 16 blocks, each lasting 60 s, with two  
210 conditions interleaved, eyes closed (EC) and eyes open (EO), starting with the EC condition.  
211 Changes between blocks were announced with the software Presentation (v16.5,  
212 Neurobehavioral Systems Inc., USA). Participants were asked to sit comfortably in a chair in  
213 a dimly illuminated, sound-shielded Faraday recording room. During the EO periods,  
214 participants were instructed to stay awake while fixating on a black cross presented on a white  
215 background. To maximize comparability, only EEG data from the EO condition were  
216 analyzed, since rsfMRI data were collected only in the EO condition.

#### 217 **2.4.EEG Data Analysis**

218 EEG processing and analyses were performed with custom Matlab (The MathWorks,  
219 Inc, Natick, Massachusetts, USA) scripts using functions from the EEGLAB environment  
220 (version 14.1.1b; Delorme and Makeig, 2004). The continuous EEG data were down-sampled  
221 to 250 Hz, band-pass filtered within 1–45 Hz (4<sup>th</sup> order back and forth Butterworth filter) and  
222 split into EO and EC conditions. Segments contaminated by large artefacts due to facial  
223 muscle tensions and gross movements were removed following visual inspection, resulting in  
224 a rejection of on average 6.6% of the recorded data. Rare occasions of artifactual channels  
225 were excluded from the analysis. The dimensionality of the data was reduced using principal  
226 component analysis (PCA) by selecting at least 30 principal components explaining 95% of  
227 the total variance. Next, using independent component analysis (Infomax; Bell and  
228 Sejnowski, 1995), the confounding sources e.g. eye-movements, eye-blanks, muscle activity,  
229 and residual ballistocardiographic artefacts were rejected from the data.

#### 230 **2.5.EEG Source Reconstruction**

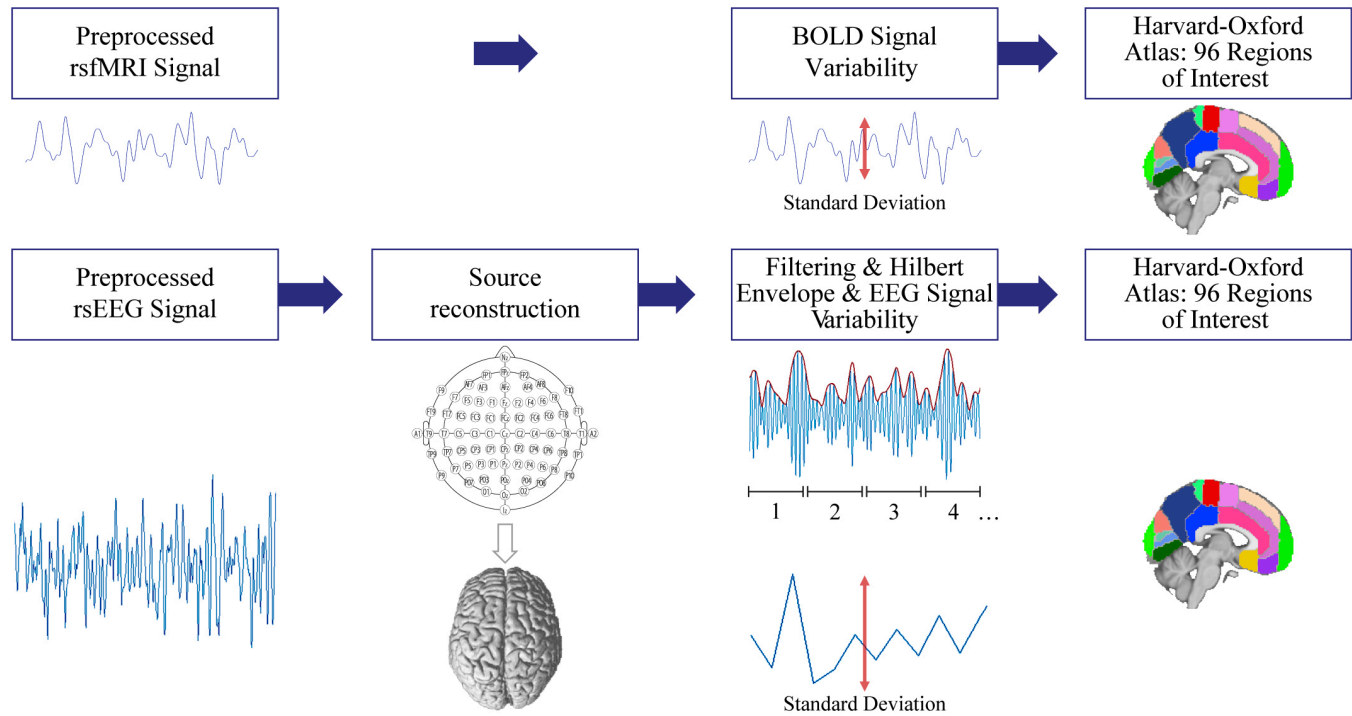
231 Before conducting source reconstruction, preprocessed EEG signals were re-  
232 referenced to a common average. We incorporated a standard highly detailed finite element  
233 method (FEM) volume conduction model as described by Huang et al. (2016).  
234 The geometry of the FEM model was based on an extended MNI/ICBM152 (International  
235 Consortium for Brain Mapping) standard anatomy, where the source space constrained to  
236 cortical surface and parceled to 96 ROIs based on the Harvard-Oxford atlas (Desikan et al.,  
237 2006). We used eLORETA (exact low resolution brain electromagnetic tomography) as  
238 implemented in as implemented in as implemented in the M/EEG Toolbox of Hamburg  
239 (METH; Haufe and Ewald, 2016; Pascual-Marqui, 2007) to compute the cortical electrical  
240 distribution from the scalp EEG recordings. The leadfield matrix was calculated between

241 1804 points located on the cortical surface to the 61 scalp electrodes. We filtered into several  
242 frequency bands, associated with brain oscillations: delta (1–3 Hz), theta (4–8 Hz), alpha (8–  
243 12 Hz), and beta (15–25 Hz). Following the singular value decomposition (SVD) of each  
244 voxel's three-dimensional time course, the dominant orientation of the source signal was  
245 identified by preserving the first SVD component. The amplitude envelope of filtered  
246 oscillations was extracted using the Hilbert transform (Rosenblum et al., 2001). Next, we  
247 applied temporal coarse graining by averaging data points in non-overlapping windows of  
248 length 0.5 s (Figure 1).

249 *EEG Variability (SD<sub>EEG</sub>)*. We calculated the SD of amplitude envelope of band-pass filtered  
250 oscillations on the coarse-grained signal. RsEEG signal variability (SD<sub>EEG</sub>) was obtained for  
251 different frequency bands (SD<sub>DELTA</sub>, SD<sub>THETA</sub>, SD<sub>ALPHA</sub>, SD<sub>BETA</sub>) in each of 96 ROIs. Further,  
252 in our study we investigated variability in the amplitude of oscillatory signals from one time  
253 segment to the other. If amplitude (or power) of each signal stays the same, the variability  
254 (SD) in the amplitude of such segments will be zero. Therefore, the average amplitude of a  
255 signal is not indicative of its variability. Although amplitude and its standard deviation  
256 mathematically are different, they can show some correlation due to size effects (Immer,  
257 1937).

258 Main steps toward deriving brain signal variability from the preprocessed EEG signal are  
259 shown in Figure 1. The raw and preprocessed fMRI and EEG data samples can be found at  
260 [https://ftp.gwdg.de/pub/misc/MPI-Leipzig\\_Mind-Brain-Body-LEMON/](https://ftp.gwdg.de/pub/misc/MPI-Leipzig_Mind-Brain-Body-LEMON/)

261 **Figure 1.** Main steps of deriving brain signal variability from the preprocessed resting state  
262 fMRI and EEG signal. We calculated the standard deviation of the blood oxygen level  
263 dependent (BOLD) signal and of the coarse-grained amplitude envelope of the rsEEG time  
264 series for a number of standard frequency bands at the source space. Each sample of coarse-  
265 grained amplitude envelope of the rsEEG (represented in numbers) is generated by averaging  
266 the samples in non-overlapping windows of length 0.5 s.



267

268

## 269 **2.6. Statistical Analyses**

270 *Mean  $SD_{BOLD}$  and  $SD_{EEG}$ .* For the topographic information (based on ROIs), the mean BOLD  
271 and EEG variability were calculated by I) log-transforming the SD values, II) averaging  
272 separately for younger and older subjects, and III) then back-transforming the values  
273 (McDonald, 2014).

274

275 *Age and Sex Effects.* A series of non-parametric analyses of covariance (ANCOVAs, type III)  
276 were applied to brain signal variability values in each 96 ROIs for  $SD_{BOLD}$  and  $SD_{EEG}$  using  
277 age group and sex as variables of interest, adjusting for TIV and mean FD. The significance  
278 level was controlled for using false discovery rate (FDR) correction according to Benjamini  
279 and Hochberg (1995). Significant group differences were further examined by Tukey HSD  
280 post-hoc comparisons. The signal variability values were log-transformed to normalize  
281  $SD_{BOLD}$  and  $SD_{EEG}$  before further analyses (assessed by Lilliefors tests at a significance

282 threshold of 0.05). All analyses were performed using the *aovp* function in the *lmpem*  
283 package (Wheeler, 2016) as implemented in R (R core team, 2018).

284

285 *SD<sub>BOLD</sub> – SD<sub>EEG</sub> Correlation*. To investigate the association between each ROI of SD<sub>BOLD</sub> and  
286 SD<sub>EEG</sub>, we used pairwise Spearman's rank correlation separately for younger and older  
287 subjects, corrected for FDR (96 ROIs). We further applied sparse canonical correlation  
288 analysis (CCA) to show that the relationship between SD<sub>BOLD</sub> and SD<sub>EEG</sub> is not missed when  
289 only mass bivariate correlations are used. CCA is a multivariate method to find the  
290 independent linear combinations of variables such that the correlation between variables is  
291 maximized (Witten et al., 2009). The sparse CCA criterion is obtained by adding a Lasso  
292 Penalty function ( $l_1$ ), which performs continuous shrinkage and automatic variable selection  
293 and can solve statistical problems such as multicollinearity and overfitting (Tibshirani, 2011).  
294 We used  $l_1$  penalty as the regularization function to obtain sparse coefficients, that is, the  
295 canonical vectors (i.e., translating from full variables to a data matrix's low-rank components  
296 of variation) will contain exactly zero elements. Sparse CCA was performed using the R  
297 package PMA (Penalized Multivariate Analysis; Witten et al., 2009; [http://cran.r-  
298 project.org/web/packages/PMA/](http://cran.r-project.org/web/packages/PMA/)). In our analyses, the significance of the correlation was  
299 estimated using the permutation approach (N=1000) as implemented in the CCA.permute  
300 function in R ( $p_{perm} < 0.05$ ).

301

302 *Cognition*. The Trail Making Test (TMT) is a cognitive test measuring executive function,  
303 including processing speed and mental flexibility (Reitan, 1955; Reitan and Wolfson, 1995).  
304 In the first part of the test (TMT-A) the targets are all numbers, while in the second part  
305 (TMT-B), participants need to alternate between numbers and letters. In both TMT-A and B,  
306 the time to complete the task quantifies the performance, and lower scores indicate better  
307 performance. Based on the previous literature, we focused on SD<sub>BOLD</sub>, SD<sub>DELTA</sub>, and SD<sub>THETA</sub>  
308 (Vlahou et al., 2015) and selected different ROIs from two research papers about the neural  
309 correlates of the TMT: Zakzanis et al., (2005) and Jacobson et al., (2011) (Table 1). To reduce  
310 the number of multiple comparisons (Nguyen and Holmes, 2019), these ROIs were  
311 decomposed into singular values using the *prcomp* function belonging to *factoextra* package  
312 (R core team, 2018), which performs SVD on the centered values. As a criterion, the  
313 minimum total variance explained over 70% was selected (Jolliffe and Cadima, 2016). This  
314 resulted in three principle components (PC) in SD<sub>BOLD</sub> (52.82%, 10.34%, and 7%), two PCs  
315 in SD<sub>DELTA</sub> (67.37%, 10.95%), and one PC in SD<sub>THETA</sub> (75.63%). We also ran multiple linear

316 regression using task completion time in TMT-A and TMT-B as the dependent variables with  
317 the PC scores (for  $SD_{BOLD}$ ,  $SD_{DELTA}$ , and  $SD_{THETA}$ ) and their interaction with continuous age  
318 as independent variables. Since the residuals from the regression models fitted to the data  
319 were not normally distributed, the TMT values were log-transformed prior to the final  
320 analyses. These tests were conducted using the *lmp* function in *lmp* package implemented  
321 in R (R core team, 2018).

322

323 **Table 1.** Selected region of interests (ROIs) derived from the previous fMRI literature, and  
324 their corresponding ROIs in Harvard-Oxford atlas to investigate the age-dependent  
325 relationship between TMT and  $SD_{BOLD}$  or  $SD_{EEG}$ .

<b>Literature</b>	<b>Region</b>	<b>Hemisphere</b>	<b>Harvard-Oxford Atlas</b>
Zakzanis et al., 2005	Middle Frontal Gyrus	Left	Middle Frontal Gyrus
	Precentral Gyrus	Left	Precentral Gyrus
	Cingulate Gyrus	Left/Right	Cingulate Gyrus, anterior/posterior
	Superior Frontal Gyrus	Left	Superior Frontal Gyrus
	Medial Frontal Gyrus	Left	Frontal Medial Cortex
	Insula	Left/Right	Insular Cortex
	Middle Temporal Gyrus	Left	Middle Temporal Gyrus, anterior/posterior/temporooccipital
Jacobson et al., 2011	Superior Temporal Gyrus	Left	Superior Temporal Gyrus, anterior/posterior
	Fusiform Gyrus	Right	Occipital Fusiform Gyrus
	Inferior Middle Frontal Gyrus	Right	Middle Frontal Gyrus
	Precentral Gyrus	Right	Precentral Gyrus

326

327

### 3. Results

328 *Mean SD<sub>BOLD</sub> and SD<sub>EEG</sub>.* The topographic distribution of SD<sub>BOLD</sub> in younger adults revealed  
329 the largest brain signal variability values in fronto-temporal regions while in older adults it  
330 was in the frontal and occipital areas. Further, we found strongest variability across younger  
331 subjects in occipito-temporal regions for SD<sub>DELTA</sub>, SD<sub>THETA</sub>, SD<sub>ALPHA</sub>, and in medial frontal  
332 brain regions for SD<sub>BETA</sub>, while older adults showed strongest brain signal variability in the  
333 fronto-central brain regions for SD<sub>DELTA</sub>, in parietal-central brain regions for SD<sub>THETA</sub>,  
334 SD<sub>ALPHA</sub>, and in medial frontal brain regions for SD<sub>BETA</sub>. The details of the mean values of  
335 SD<sub>BOLD</sub> and SD<sub>EEG</sub> across age groups and their topographic distributions are given in  
336 Supplementary Table 1, Supplementary Figure 2 and 3, and are also available at Neurovault  
337 (<https://neurovault.org/collections/WWOKVUDV/>).

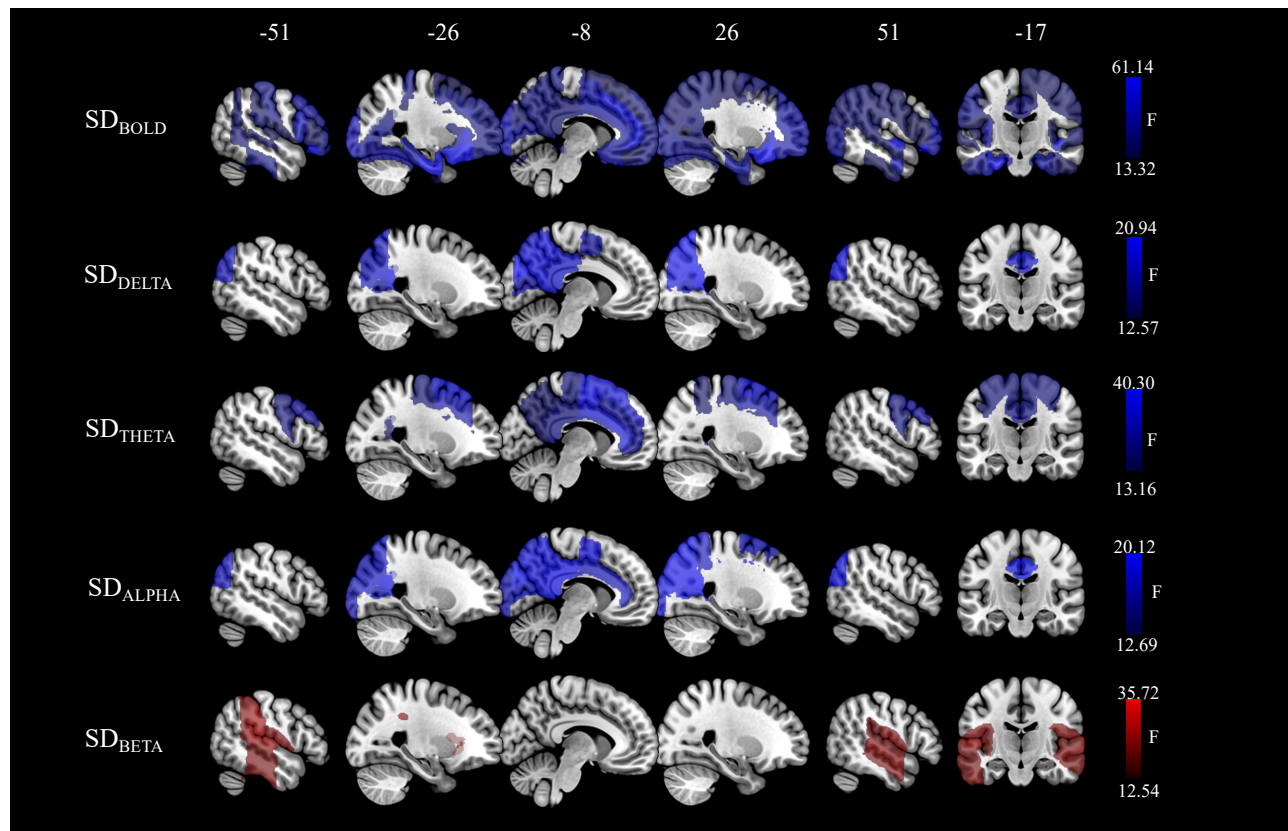
338

339 *Age and Sex Effects.* The nonparametric ANCOVAs with SD<sub>BOLD</sub> as dependent variable  
340 demonstrated that there was a significant main effect of age group in 72 ROIs in frontal,  
341 temporal, and occipital brain regions (F-values: 13.32–61.14; Figure 2). However, there was  
342 no significant main effect of sex on SD<sub>BOLD</sub> and no significant interaction between age group  
343 and sex (all  $p_{FDR} > 0.05$ ). Tukey HSD post-hoc analyses showed that older subjects had  
344 decreased SD<sub>BOLD</sub> compared to younger adults which were presented in both sexes ( $n_{ROI} = 35$ ).  
345 The nonparametric ANCOVAs with SD<sub>EEG</sub> as dependent variable showed significant main  
346 effects of age group in all frequency bands: SD<sub>DELTA</sub> in 14 ROIs in occipital (F-values: 12.57–  
347 20.94), SD<sub>THETA</sub> in 16 ROIs in frontal and parietal (F-values: 13.16–40.30), SD<sub>ALPHA</sub> in 20  
348 ROIs in occipital (F-values: 12.69–20.12), and SD<sub>BETA</sub> in 19 ROIs in central and temporal  
349 brain regions (F-values: 12.50–21.61), as shown in Figure 2. There were also significant main  
350 effects of sex in all frequency bands: SD<sub>DELTA</sub> in 21 ROIs in temporal and occipital (F-values:  
351 13.24–26.63), SD<sub>THETA</sub> in 74 ROIs in frontal, occipital, and temporal (F-values: 12.68–30.06),  
352 SD<sub>ALPHA</sub> in 4 ROIs in frontal (F-values: 12.88–16.51), and SD<sub>BETA</sub> in 69 ROIs in temporal,  
353 occipital, and central brain regions (F-values: 12.54–35.72), as shown in Figure 3. No  
354 significant interaction effects between age group and sex on SD<sub>EEG</sub> were observed in any  
355 frequency band ( $p_{FDR} > 0.05$ ). Tukey HSD post-hoc analyses on SD<sub>EEG</sub> showed that older  
356 subjects had less brain signal variability, which was present in both sexes for SD<sub>DELTA</sub>  
357 ( $n_{ROI} = 12$ ), SD<sub>THETA</sub> ( $n_{ROI} = 10$ ), and SD<sub>ALPHA</sub> ( $n_{ROI} = 11$ ). Additionally, older adults showed  
358 higher SD<sub>BETA</sub>, driven by female subjects ( $n_{ROI} = 15$ ). With regard to sex differences, post-hoc  
359 analyses showed that females had higher SD<sub>DELTA</sub>, SD<sub>THETA</sub>, SD<sub>ALPHA</sub>, and SD<sub>BETA</sub> than  
360 males. Sex differences in SD<sub>DELTA</sub> ( $n_{ROI} = 13$ ) and SD<sub>THETA</sub> ( $n_{ROI} = 54$ ) were mostly pronounced

361 in younger adults, while the effect of sex in  $SD_{BETA}$  ( $n_{ROI}=21$ ) were mainly presented in older  
362 adults ( $p<0.05$ ). The graphical distribution of the F-values for the significant effects of age  
363 group or sex for each ROIs are shown in Supplementary Figure 4. Additional information of  
364  $SD_{BOLD}$  and  $SD_{EEG}$  for each frequency band and for each of the 96 ROIs, split up by age group  
365 and sex, are presented in the Supplementary Tables 2-6.

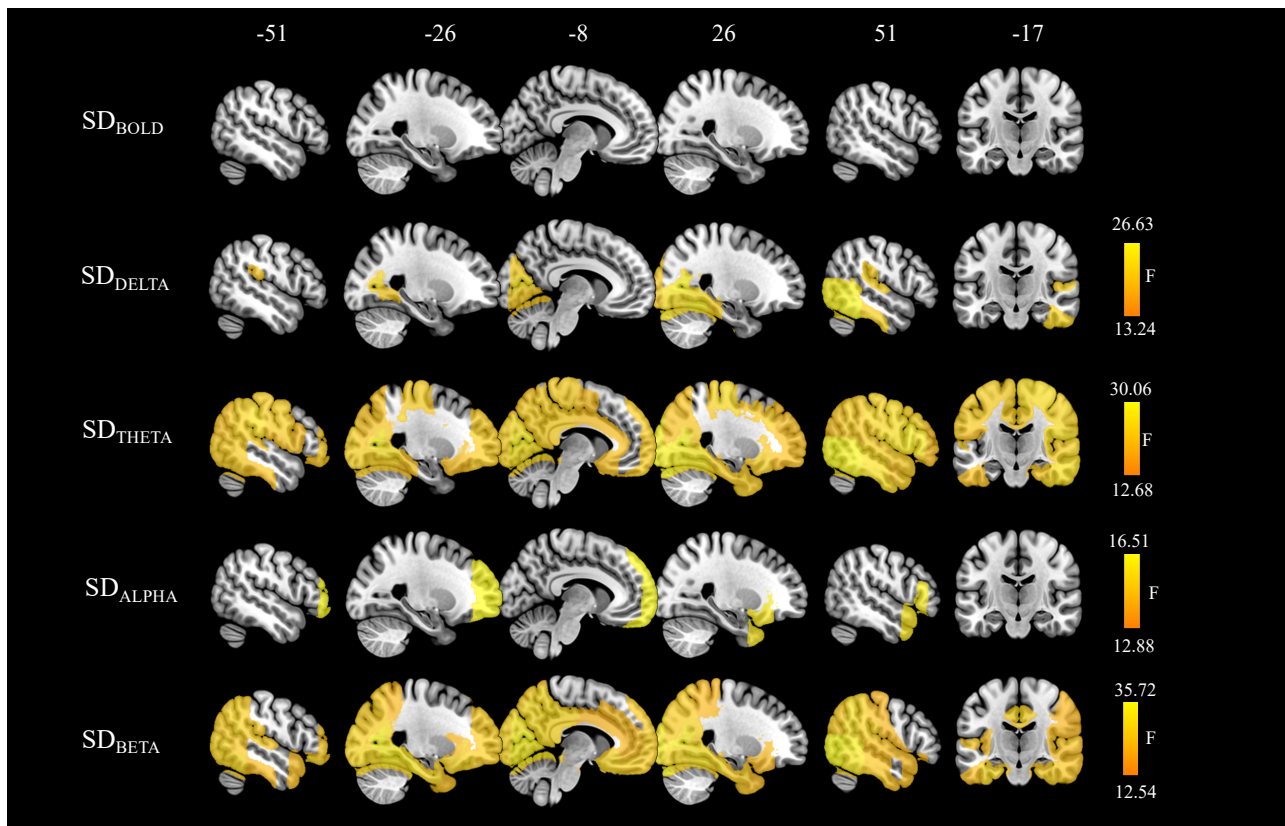
366

367 **Figure 2.** Spatial maps of significant age group differences in  $SD_{BOLD}$  and  $SD_{EEG}$ .  
368 We calculated the standard deviation (SD) of the blood oxygen level dependent (BOLD)  
369 signal and of the coarse-grained amplitude envelope of the rsEEG time series for the delta (1–  
370 3 Hz), theta (4–8 Hz), alpha (8–12 Hz), and beta (15–25 Hz) frequency bands at the source  
371 space. Statistical significance was determined using nonparametric ANCOVAs corrected for  
372 multiple comparisons by false discovery rates (FDR; Benjamini and Hochberg, 1995). Blue  
373 color indicates areas where brain signal variability was lower in older than in younger adults,  
374 while red color indicates the opposite.



375

376 **Figure 3.** Spatial maps of significant sex differences in  $SD_{BOLD}$  and  $SD_{EEG}$ .  
377 We calculated the standard deviation (SD) of the blood oxygen level dependent (BOLD)  
378 signal and of the coarse-grained amplitude envelope of the rsEEG time series for the delta (1–  
379 3 Hz), theta (4–8 Hz), alpha (8–12 Hz), and beta (15–25 Hz) frequency bands at the source  
380 space. Statistical significance was determined using nonparametric ANCOVAs corrected for  
381 multiple comparisons by false discovery rates (FDR; Benjamini and Hochberg, 1995). Yellow  
382 color indicates areas where brain signal variability was higher in female subjects as compared  
383 to male subjects in EEG.

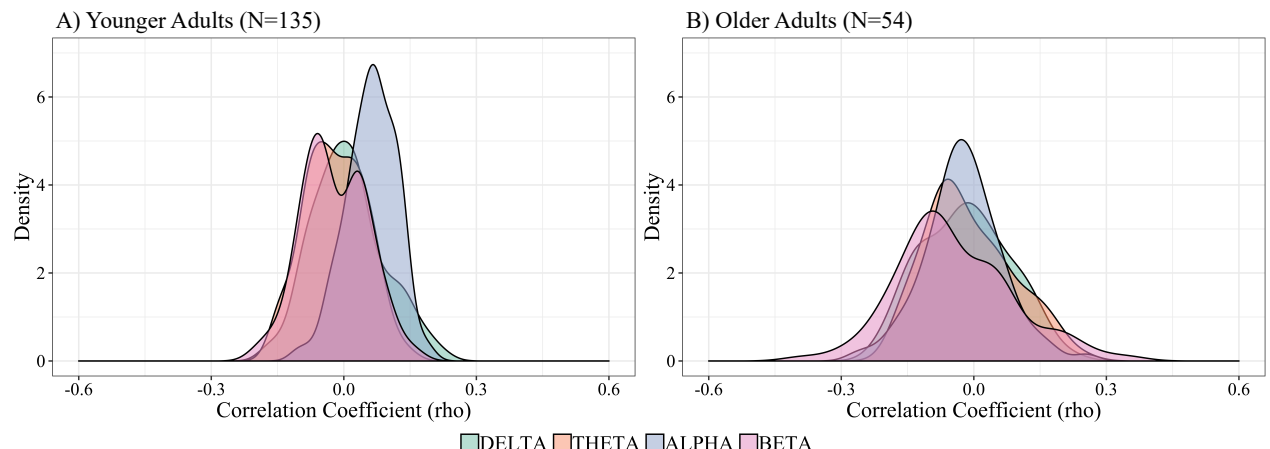


384

385  $SD_{BOLD} - SD_{EEG}$  Correlation. The correlation coefficient of pairwise associations for 96 ROIs  
386 of  $SD_{BOLD}$  with  $SD_{\text{DELTA}}$ ,  $SD_{\text{THETA}}$ ,  $SD_{\text{ALPHA}}$ , and  $SD_{\text{BETA}}$  ranged in younger adults from  $\rho = -0.200$  to  $\rho = 0.223$  (Supplementary Table 7) and in older adults from  $\rho = 0.386$  to  
387  $\rho = 0.349$  (Supplementary Table 8). None of the pairwise associations between  $SD_{BOLD}$  and  
388  $SD_{EEG}$  remained significant after the correction for multiple comparison corrections.  
389 Confirmatory multivariate sparse CCA further showed that correlations between  $SD_{BOLD}$  and  
390  $SD_{EEG}$  across all subjects were rather low, highly sparse, and non-significant ( $SD_{\text{DELTA}}$ ;  
391  $r = 0.145$ ,  $p_{\text{perm}} = 0.750$ ,  $l_1 = 0.367$ ;  $SD_{\text{THETA}}$ ;  $r = 0.143$ ,  $p_{\text{perm}} = 0.713$   $l_1 = 0.7$ ;  $SD_{\text{ALPHA}}$ ;  $r = 0.153$ ,  
392  $p_{\text{perm}} = 0.528$ ,  $l_1 = 0.1$ ;  $SD_{\text{BETA}}$ ;  $r = 0.232$ ,  $p_{\text{perm}} = 0.096$ ,  $l_1 = 0.633$ ).  
393

394

395 **Figure 4.** Distribution of correlation coefficients ( $\rho$ ) for the association between  $SD_{BOLD}$   
396 and  $SD_{EEG}$  for A) younger ( $N=135$ ) and B) older ( $N=54$ ) adults for different frequency bands  
397 across each pair of 96 regions of interests. The correlations between  $SD_{BOLD}$  and  $SD_{EEG}$  were  
398 tested using pairwise Spearman's rank correlation corrected for multiple comparison by false  
399 discovery rates (FDR; Benjamini and Hochberg, 1995).



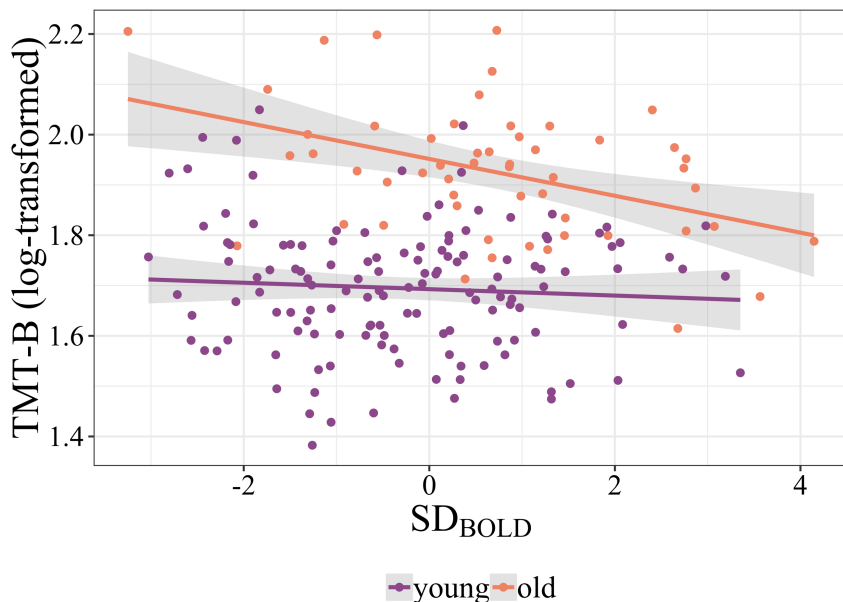
400

401 *Cognition.* There was a significant interaction between age and  $SD_{BOLD}$  in PC2 on the TMT-B  
402 performance (adjusted  $R^2 = 0.395$ ,  $F(7,181) = 18.60$ ,  $p < .001$ , interaction:  $\beta = -0.002$ ,  $p =$   
403 0.027). For older, but not younger participants, stronger  $SD_{BOLD}$  was associated with faster  
404 completion time in PC2, driven mainly by the left temporal gyrus as well as the left anterior  
405 and posterior cingulate cortex (Figure 5). The regression analyses in  $SD_{\text{DELTA}}$  and  $SD_{\text{THETA}}$   
406 did not show a significant association between cognition and brain signal variability  
407 measures. The contributions of selected ROIs to the PCs resulted from SVD analyses can be  
408 found in Supplementary Table 9. The complete multiple linear regression results can be found  
409 in Supplementary Table 10.

410

411 **Figure 5.** Age-dependent relationship between cognitive performance and BOLD signal  
412 variability.

413 The scatterplot shows the significant association between task completion time in TMT-B (x-  
414 axis) and  $SD_{BOLD}$  (adjusted  $R^2 = 0.395$ ,  $F(7,181) = 18.60$ ,  $p < .001$ , interaction:  $\beta = -0.002$ ,  $p =$   
415 0.027) in PC2, driven mainly by the left anterior and posterior temporal gyrus, bilateral  
416 anterior and posterior cingulate cortex.



417

418

419

#### 4. Discussion

420 Comparing healthy younger and older adults, we found widespread variability  
421 reductions in BOLD signal as well as in the amplitude envelope of delta, theta, and alpha  
422 frequency of rsEEG, whereas increased variability with aging was observed in the beta-band  
423 frequency. As a complementary analysis, we also explored sex differences and found that  
424 female subjects exhibited higher EEG signal variability than male subjects; no significant sex  
425 differences were found in BOLD signal variability. There were no significant correlations  
426 between hemodynamic ( $SD_{BOLD}$ ) and electrophysiological ( $SD_{EEG}$ ) measures of brain signal  
427 variability, neither in the younger nor in the older adults. Our results suggest that variability  
428 measures of rsfMRI and rsEEG – while both related to aging – are dominated by different  
429 physiological origins and relate differently to age and sex.

430

431

##### 4.1.BOLD Signal Variability

432 The first aim of our study was to investigate the effect of age on BOLD signal  
433 variability, as measured by SD of spontaneous fluctuations during rsfMRI. Consistent with  
434 recent rsfMRI studies demonstrating that BOLD signal variability decreases with age in large-  
435 scale networks (Grady and Garrett, 2018; Nomi et al., 2017), we found that older subjects had  
436 reduced  $SD_{BOLD}$  in temporal and occipital brain regions but also in cortical midline structures  
437 like the precuneus, anterior and posterior cingulate cortices, as well as orbitofrontal cortex  
438 compared to younger adults. These age-related reductions in BOLD signal variability were  
439 thus especially apparent in regions of the Default Mode (DMN) and the Fronto-Parietal  
440 Network (FPN). The DMN is an intrinsically correlated network of brain regions, that is  
441 particularly active during rest or fixation blocks (Biswal et al., 2010). It reflects the systematic  
442 integration of information across the cortex (Margulies et al., 2016) and has been frequently  
443 associated with psychological functions like self-referential thought or mind-wandering, and  
444 also memory retrieval (Andrews-Hanna et al., 2014; Raichle, 2015). The FPN is involved in  
445 cognitive control processes (Spreng et al., 2013), and closely interacts with the DMN, for  
446 example during mind-wandering state (Golchert et al., 2017). Previous studies in healthy  
447 aging noted that older subjects showed lower functional connectivity in DMN and FPN  
448 regions (Damoiseaux, 2017; Damoiseaux et al., 2008; Meunier et al., 2009; Petersen et al.,  
449 2014). Similarly, an altered functional connectivity in the DMN has been found in different  
450 pathologies, for example, in Alzheimer's disease (Greicius et al., 2004) or mild cognitive  
451 impairment (Das et al., 2015). Further, we found a significant interaction between age and  
452  $SD_{BOLD}$  in temporal and cingulate cortices for performance on the cognitive task (TMT-B),

453 suggesting that the relationship between brain signal variability and cognitive performance  
454 depends on the participants' age. We speculate that – in the elderly – reduced BOLD signal  
455 variability in the DMN and the FPN, particularly in the overlapping frontal brain regions,  
456 could be related to locally impaired function that is reflected in impaired cognitive  
457 performance (Campbell et al., 2012). Such findings support the notion that local BOLD signal  
458 variability may be a valuable biomarker of neurocognitive health (and disease) in aging.

459 Sex-specific differences in brain structure and function have been previously shown  
460 (for a review see, Gong et al., 2011; Ruigrok et al., 2014; Sacher et al., 2013). For example,  
461 larger total brain volume has been reported in male as compared to female subjects (Gong et  
462 al., 2011), whereas higher cerebral blood flow (Gur et al., 1982; Rodriguez et al., 1988) and  
463 stronger functional connectivity in the DMN (Tomasi and Volkow, 2012) were found in  
464 females. In our exploratory analysis, we did not find significant sex differences in BOLD  
465 signal variability when controlling for total intracranial volume as an approximation of overall  
466 brain size.

467

#### 468 **4.2.Electrophysiological Signal Variability**

469 Measures of neural variability were derived from rsEEG for several main frequency  
470 bands (delta, theta, alpha, beta) as the standard deviation of their amplitude of envelope time  
471 series data, analogously to the BOLD signal variability. Multimodal imaging studies have  
472 shown that the amplitude envelope of neural oscillatory activity across frequency bands  
473 relates to different rsfMRI networks (Brookes et al., 2011; Deligianni et al., 2014), confirming  
474 the neurophysiological origin of the resting state networks measured with BOLD fMRI.  
475 Additionally, these studies also concluded that different frequency bands can be related to the  
476 same functional network, but also differentially to distinct networks (Brookes et al., 2011;  
477 Laufs et al., 2006; Mantini et al., 2007; Meyer et al., 2013). For instance, Mantini et. al.  
478 (2007) reported that the visual network is associated with all frequency bands except gamma  
479 rhythm, while the sensorimotor network is primarily associated with beta-band oscillations.

480 In our analysis, we found age-dependent EEG signal variability changes within  
481 networks which were associated with more than one frequency band, thus confirming that  
482 neurons generating oscillations at different frequencies may contribute to the same network.  
483 More precisely, we found age-related reductions in SD<sub>DELTA</sub> and SD<sub>ALPHA</sub> mainly in a visual  
484 network (including calcarine regions, cuneal cortex, and occipital pole), SD<sub>THETA</sub> in posterior  
485 DMN (e.g., posterior cingulate cortex), while an enhancement of SD<sub>BETA</sub> was mainly seen in  
486 the temporal (e.g., superior/middle temporal gyrus), and central/sensorimotor (e.g.,

487 supramarginal gyrus) regions. These results align with previous reports of age-dependent  
488 changes of electrophysiological activity using spectral power (Dustman et al., 1993; Vlahou et  
489 al., 2015), and signal variability (Dustman et al., 1999; Tsvetanov et al., 2015).

490 Age-related decreases of alpha amplitude and alpha band variability (measured by SD  
491 of the oscillatory signal) were previously found in posterior and occipital brain regions  
492 (Babiloni et al., 2006; Tsvetanov et al., 2015). Alpha rhythm is a classical EEG hallmark of  
493 resting wakefulness (Laufs et al., 2003) that is modulated by thalamo-cortical and cortico-  
494 cortical interactions (Bazanova and Vernon, 2014; Goldman et al., 2002; Lopes Da Silva et  
495 al., 1997; Moosmann et al., 2003). It has been suggested that the posterior alpha-frequency  
496 plays an important role in the top-down control of cortical activation and excitability  
497 (Klimesch, 1999). Accordingly, decreased alpha variability in occipital regions might be  
498 associated with altered functioning of the cholinergic basal forebrain, affecting thalamo-  
499 cortical and cortico-cortical processing. Our finding of higher temporal and sensorimotor  
500 SD<sub>BETA</sub> in the elderly is in line with previous findings (Rossiter et al., 2014; Tsvetanov et al.,  
501 2015). Aging has previously been associated with an increase in movement-related beta-band  
502 attenuation, suggesting an enhanced motor cortex GABAergic inhibitory activity in older  
503 individuals (Rossiter et al., 2014). Similarly, beta-band activity is thought to play a key role in  
504 signaling maintenance of the status quo of the motor system, despite the absence of  
505 movement (Engel and Fries, 2010). Therefore, greater SD<sub>BETA</sub> in sensorimotor brain regions  
506 could be interpreted as a compensatory mechanism to account for a decline of motor  
507 performance during aging (Quandt et al., 2016).

508 It should be noted that the present findings of age-related alterations of brain signal  
509 variability at different frequencies might be influenced by several anatomical factors which  
510 might influence EEG-generators such as reduced cortical gray matter (Babiloni et al., 2013;  
511 Moretti et al., 2012), white-matter (Nunez et al., 2015; Valdés-Hernández et al., 2010), and  
512 increased amount of cerebrospinal fluid (CSF; Hartikainen et al., 1992; Stomrud et al., 2010),  
513 but also alterations of cerebral glucose metabolism (Dierks et al., 2000). Localized or global  
514 disturbances of brain anatomy and function might lead to deviations in the EEG sources,  
515 resulting in EEG amplitude changes. A methodological improvement for future studies will  
516 therefore be the application of individual head models (Ziegler et al., 2014).

517 In addition to the effect of age on rsEEG signal variability, an exploratory analysis  
518 showed sex differences in distinct brain regions and EEG frequencies. More precisely, we  
519 found higher SD<sub>DELTA</sub> and SD<sub>THETA</sub> in occipito-temporal, SD<sub>ALPHA</sub> in frontal, and SD<sub>BETA</sub> in  
520 frontal as well as occipito-temporal brain regions in female compared to male subjects. While

521 some studies demonstrated higher alpha (Auriel et al., 2003), delta (Armitage, 1995), theta  
522 (Carrier et al., 2001; Duffy et al., 1993), and beta power (Jaušovec and Jaušovec, 2010;  
523 Matsuura et al., 1985; Veldhuizen et al., 1993) in female relative to male subjects, other  
524 studies reported the opposite pattern (Brenner et al., 1995; Latta et al., 2005; Zappasodi et al.,  
525 2006). These differences in EEG signal variability could be a result of different mechanisms  
526 (biological/hormonal, cultural or developmental) involved in shaping sex differences.  
527 Unfortunately, based on our dataset we cannot differentiate which of these potential  
528 mechanisms might be most relevant for the observed changes.

529

### 530 **4.3. Association between BOLD and EEG Variability**

531 We further assessed how neural variability in source-reconstructed rsEEG related to  
532 the analogous parameters of BOLD signal variability in rsfMRI using univariate and  
533 multivariate correlation analyses. Previously, simultaneous EEG-fMRI studies have shown  
534 meaningful relationships between fluctuations in EEG power, frequency, phase, and local  
535 BOLD changes (for a review see, Jorge et al., 2014; Ritter and Villringer, 2006). Due to age-  
536 related physiological (particularly cardiovascular) alterations in the brain, we expected the  
537 relationship between BOLD and EEG signal variability to be stronger in younger than older  
538 adults. However, in the present study, both univariate and multivariate analyses showed no  
539 significant correlations between  $SD_{BOLD}$  and  $SD_{EEG}$  neither in the younger nor in the older  
540 adults. This finding was supported by the distinct anatomical distributions of age-related  
541 changes in BOLD and EEG signal variability, that barely showed a spatial overlap, suggesting  
542 different underlying physiological processes. What could they be? Clearly, neuronal activity  
543 is the main signal source for EEG- and MEG recordings as well as for EEG/MEG-based  
544 variability measures. BOLD signal variability, however, can reflect both vascular and neural  
545 processes (Garrett et al., 2017). While neuronal activity clearly contributes to the BOLD  
546 signal at rest (Ma et al., 2016; Mateo et al., 2017), our results indicate, however, that neuronal  
547 activity which is captured by EEG (or more specifically by our EEG-based measures), is not  
548 the major determinant of BOLD variability in the resting state. Other factors that could  
549 contribute to BOLD variability are (i) neuronal activity which is not captured by EEG and (ii)  
550 non-neuronal factors such as vasomotion, or cardiac and respiratory signals (Murphy et al.,  
551 2013). In the elderly, additional factors related to the known morphological and functional  
552 changes of blood vessels as well as age-related metabolic changes are known to affect CBF  
553 (Ances et al., 2009; Martin et al., 1991), CMRO<sub>2</sub> (Aanerud et al., 2012), and CVR (Liu et al.,  
554 2013) and therefore are likely to also influence BOLD variability. Thus, given different

555 underlying physiology, joint EEG and fMRI variability studies might provide complementary  
556 information for a comprehensive assessment of neuronal as well as vascular factors related to  
557 aging.

## 558 5. Limitations

559 There are several limitations of our study: EEG and MRI scans were not recorded  
560 simultaneously. Therefore, we could not directly relate the two signals in a cross-correlation  
561 analysis. Furthermore, EEG and MRI were performed with different body postures (fMRI;  
562 supine, EEG; seated) known to affect brain function, for example, changes in the amplitude of  
563 the EEG signal have been related to different body postures presumably due to the shifts in  
564 cerebrospinal fluid layer thickness (Rice et al., 2013). Similarly, other experimental (e.g.,  
565 visual display; Nir et al., 2006), environmental (e.g., acoustic noise in MRI; Andoh et al.,  
566 2017; Cho et al., 1998) and subject-related factors (e.g., changes of vigilance; Tagliazucchi  
567 and Laufs, 2014; Wong et al., 2013) could have introduced unintended variations in our  
568 results (Yan et al., 2013) and the influence of these factors is probably not the same for the  
569 different methods, e.g., noise in MRI or poor “control” of vigilance in MRI. For instance,  
570 given the well-known relationship between vigilance or arousal and fMRI signal fluctuations  
571 (Bijsterbosch et al., 2017; Chang et al., 2016; Haimovici et al., 2017), it is likely that the  
572 observed age-related differences in BOLD signal variability might be confounded by such  
573 within-subject (state) variability. Therefore, future rsfMRI studies may benefit from obtaining  
574 arousal-related (e.g., self-report) measures and an explicit measurement of eye movements  
575 and eye opening/closure to account for the influence of arousal on the BOLD amplitude  
576 changes. Another option would be to combine EEG and fMRI simultaneously. Yet, resting  
577 state measures of EEG (Näpflin et al., 2007) and fMRI (Shehzad et al., 2009; Zuo et al., 2010)  
578 have been shown to be reliable within-individuals across time.

579 In our study, the computation of the source reconstructed rsEEG required the  
580 parcellation of the brain into relatively large anatomical ROIs. It could well be that the  
581 analysis with a higher spatial resolution (e.g., at the voxel-level) with individual head models  
582 may provide additional insights about brain signal variability.

583 Finally, while our study aimed at comparing analogous variability measures in EEG  
584 and fMRI, future research using rsEEG and rsfMRI in the same subjects would benefit from  
585 the addition of connectivity-based measures including graph theory-based (Yu et al., 2016) or  
586 sliding-window methods (Chang et al., 2013; Qin et al., 2019).

587

## 6. Conclusion

588 In this study, we report age and sex differences of brain signal variability obtained  
589 with rsfMRI and rsEEG from the same subjects. We demonstrate extensive age-related  
590 reduction of  $SD_{BOLD}$ ,  $SD_{DELTA}$ ,  $SD_{THETA}$ , and  $SD_{ALPHA}$  mainly in the DMN and the visual  
591 network, while a significant increase of  $SD_{BETA}$  was mainly seen in temporal brain regions.  
592 We could not demonstrate significant associations between  $SD_{BOLD}$  and  $SD_{EEG}$ . Our findings  
593 indicate that measurements of BOLD and EEG signal variability, respectively, are likely to  
594 stem from different physiological origins and relate differentially to age and sex. While the  
595 two types of measurements are thus not interchangeable, it seems, however, plausible that  
596 both markers of brain variability may provide complementary information about the aging  
597 process.

598

## 7. Funding

599 This research did not receive any specific grant from funding agencies in the public,  
600 commercial, or not-for-profit sectors.

## 601 8. Acknowledgements

602 We gratefully acknowledge the Mind-Body- Emotion group at the Max Planck Institute for  
603 Human Cognitive and Brain Sciences.

## 9. References

604

605 Aanerud, J., Borghammer, P., Mallar Chakravarty, M., Vang, K., Rodell, A.B., Jónsdóttir, K.Y.,  
606 Møller, A., Ashkanian, M., Vafaei, M.S., Iversen, P., Johannsen, P., Gjedde, A., 2012. Brain  
607 energy metabolism and blood flow differences in healthy aging. *J. Cereb. Blood Flow Metab.*  
608 <https://doi.org/10.1038/jcbfm.2012.18>

609 Ances, B.M., Liang, C.L., Leontiev, O., Perthen, J.E., Fleisher, A.S., Lansing, A.E., Buxton, R.B.,  
610 2009. Effects of aging on cerebral blood flow, oxygen metabolism, and blood oxygenation level  
611 dependent responses to visual stimulation. *Hum. Brain Mapp.* 30, 1120–1132.  
612 <https://doi.org/10.1002/hbm.20574>

613 Andoh, J., Ferreira, M., Leppert, I.R., Matsushita, R., Pike, B., Zatorre, R.J., 2017. How restful is it  
614 with all that noise? Comparison of Interleaved silent steady state (ISSS) and conventional  
615 imaging in resting-state fMRI. *Neuroimage* 147, 726–735.  
616 <https://doi.org/10.1016/j.neuroimage.2016.11.065>

617 Andrews-Hanna, J.R., Smallwood, J., Spreng, R.N., 2014. The default network and self-generated  
618 thought: Component processes, dynamic control, and clinical relevance. *Ann. N. Y. Acad. Sci.*  
619 1316, 29–52. <https://doi.org/10.1111/nyas.12360>

620 Armbruster-Genc, D.J.N., Ueltzhoffer, K., Fiebach, C.J., 2016. Brain Signal Variability Differentially  
621 Affects Cognitive Flexibility and Cognitive Stability. *J. Neurosci.* 36, 3978–3987.  
622 <https://doi.org/10.1523/JNEUROSCI.2517-14.2016>

623 Armitage, R., 1995. The distribution of EEG frequencies in REM and NREM sleep stages in healthy  
624 young adults. *Sleep* 18, 334–341. <https://doi.org/10.1093/sleep/18.5.334>

625 Aurlien, H., Gjerde, I., Aarseth, J., Eldøen, G., Karlsen, B., Skeidsvoll, H., Gilhus, N., 2003. EEG  
626 background activity described by a large computerized database. *Clin. Neurophysiol.* 115, 665–  
627 673. <https://doi.org/10.1016/j.clinph.2003.10.019>

628 Avants, B.B., Tustison, N.J., Song, G., Cook, P.A., Klein, A., Gee, J.C., 2011. A reproducible  
629 evaluation of ANTs similarity metric performance in brain image registration. *Neuroimage* 54,  
630 2033–2044. <https://doi.org/10.1016/j.neuroimage.2010.09.025>

631 Babayan, A., Erbey, M., Kumral, D., Reinelt, J.D., Reiter, A.M.F., Röbbig, J., Lina Schaare, H.,  
632 Uhlig, M., Anwander, A., Bazin, P.L., Horstmann, A., Lampe, L., Nikulin, V. V., Okon-Singer,  
633 H., Preusser, S., Pampel, A., Rohr, C.S., Sacher, J., Thöne-Otto, A., Trapp, S., Nierhaus, T.,  
634 Altmann, D., Arelin, K., Blöchl, M., Bongartz, E., Breig, P., Cesnaite, E., Chen, S., Cozatl, R.,  
635 Czerwonatis, S., Dambrauskaitė, G., Dreyer, M., Enders, J., Engelhardt, M., Fischer, M.M.,  
636 Forschack, N., Golchert, J., Golz, L., Guran, C.A., Hedrich, S., Hentschel, N., Hoffmann, D.I.,  
637 Huntenburg, J.M., Jost, R., Kosatschek, A., Kunzendorf, S., Lammers, H., Lauckner, M.E.,  
638 Mahjoory, K., Kanaan, A.S., Mendes, N., Menger, R., Morino, E., Näthe, K., Neubauer, J.,  
639 Noyan, H., Oligschläger, S., Panczyszyn-Trzewik, P., Poehlchen, D., Putzke, N., Roski, S.,  
640 Schaller, M.C., Schieferbein, A., Schlaak, B., Schmidt, R., Gorgolewski, K.J., Schmidt, H.M.,

641 Schrimpf, A., Stasch, S., Voss, M., Wiedemann, A., Margulies, D.S., Gaebler, M., Villringer, A.,  
642 2019. Data descriptor: A mind-brain-body dataset of MRI, EEG, cognition, emotion, and  
643 peripheral physiology in young and old adults. *Sci. Data* 6, 180308.  
644 <https://doi.org/10.1038/sdata.2018.308>

645 Babiloni, C., Binetti, G., Cassarino, A., Dal Forno, G., Del Percio, C., Ferreri, F., Ferri, R., Frisoni, G.,  
646 Galderisi, S., Hirata, K., Lanuzza, B., Miniussi, C., Mucci, A., Nobili, F., Rodriguez, G.,  
647 Romani, G.L., Rossini, P.M., Forno, G.D., Percio, C. Del, Ferreri, F., Ferri, R., Frisoni, G.,  
648 Galderisi, S., Hirata, K., Lanuzza, B., Miniussi, C., Mucci, A., Nobili, F., Rodriguez, G.,  
649 Romani, G.L., Rossini, P.M., 2006. Sources of cortical rhythms in adults during physiological  
650 aging: A multicentric EEG study. *Hum. Brain Mapp.* 27, 162–172.  
651 <https://doi.org/10.1002/hbm.20175>

652 Babiloni, C., Carducci, F., Lizio, R., Vecchio, F., Baglieri, A., Bernardini, S., Cavedo, E., Bozzao, A.,  
653 Buttinelli, C., Esposito, F., Giubilei, F., Guizzaro, A., Marino, S., Montella, P., Quattrocchi,  
654 C.C., Redolfi, A., Soricelli, A., Tedeschi, G., Ferri, R., Rossi-Fedele, G., Ursini, F., Scascia, F.,  
655 Vernieri, F., Pedersen, T.J., Hardemark, H.G., Rossini, P.M., Frisoni, G.B., 2013. Resting state  
656 cortical electroencephalographic rhythms are related to gray matter volume in subjects with mild  
657 cognitive impairment and Alzheimer's disease. *Hum. Brain Mapp.* 34, 1427–1446.  
658 <https://doi.org/10.1002/hbm.22005>

659 Bazanova, O.M., Vernon, D., 2014. Interpreting EEG alpha activity. *Neurosci. Biobehav. Rev.* 44, 94–  
660 110. <https://doi.org/10.1016/j.neubiorev.2013.05.007>

661 Bazin, P.L., Weiss, M., Dinse, J., Schäfer, A., Trampel, R., Turner, R., 2014. A computational  
662 framework for ultra-high resolution cortical segmentation at 7 Tesla. *Neuroimage* 93, 201–209.  
663 <https://doi.org/10.1016/j.neuroimage.2013.03.077>

664 Behzadi, Y., Restom, K., Liau, J., Liu, T.T., 2007. A component based noise correction method  
665 (CompCor) for BOLD and perfusion based fMRI. *Neuroimage* 37, 90–101.  
666 <https://doi.org/10.1016/j.neuroimage.2007.04.042>

667 Bell, A.J., Sejnowski, T.J., 1995. An Information-Maximization Approach to Blind Separation and  
668 Blind Deconvolution. *Neural Comput.* 7, 1129–1159. <https://doi.org/10.1162/neco.1995.7.6.1129>

669 Benjamini, Y., Hochberg, Y., 1995. Controlling the False Discovery Rate : A Practical and Powerful  
670 Approach to Multiple Testing Author ( s ): Yoav Benjamini and Yosef Hochberg Source :  
671 Journal of the Royal Statistical Society . Series B ( Methodological ), Vol . 57 , No . 1 Published  
672 by : J. R. Stat. Soc. 57, 289–300.

673 Bijsterbosch, J., Harrison, S., Duff, E., Alfaro-Almagro, F., Woolrich, M., Smith, S., 2017.  
674 Investigations into within- and between-subject resting-state amplitude variations. *Neuroimage*  
675 159, 57–69. <https://doi.org/10.1016/j.neuroimage.2017.07.014>

676 Birn, R.M., Murphy, K., Bandettini, P.A., 2008. The effect of respiration variations on independent  
677 component analysis results of resting state functional connectivity. *Hum. Brain Mapp.* 29, 740–

678 750. <https://doi.org/10.1002/hbm.20577>

679 Biswal, B.B., Mennes, M., Zuo, X.-N., 2010. Toward discovery science of human brain function.

680 Proc. Natl. Acad. Sci. U. S. A. 107, 4734–4739. <https://doi.org/10.1073/pnas.0911855107>

681 Brenner, R.P., Ulrich, R.F., Reynolds, C.F., 1995. EEG spectral findings in healthy, elderly men and

682 women - sex differences. *Electroencephalogr. Clin. Neurophysiol.* 94, 1–5.

683 [https://doi.org/10.1016/0013-4694\(94\)00234-C](https://doi.org/10.1016/0013-4694(94)00234-C)

684 Brookes, M.J., Woolrich, M., Luckhoo, H., Price, D., Hale, J.R., Stephenson, M.C., Barnes, G.R.,

685 Smith, S.M., Morris, P.G., 2011. Investigating the electrophysiological basis of resting state

686 networks using magnetoencephalography. *Proc. Natl. Acad. Sci.* 108, 16783–16788.

687 <https://doi.org/10.1073/pnas.1112685108>

688 Burgess, A., Gruzelier, J., 1993. Individual reliability of amplitude distribution in topographical

689 mapping of EEG. *Electroencephalogr. Clin. Neurophysiol.* 86, 219–223.

690 [https://doi.org/10.1016/0013-4694\(93\)90101-Z](https://doi.org/10.1016/0013-4694(93)90101-Z)

691 Caballero-Gaudes, C., Reynolds, R.C., 2017. Methods for cleaning the BOLD fMRI signal.

692 *Neuroimage* 154, 128–149. <https://doi.org/10.1016/j.neuroimage.2016.12.018>

693 Cabeza, R., 2001. Cognitive neuroscience of aging: Contributions of functional neuroimaging. *Scand.*

694 *J. Psychol.* 42, 277–286. <https://doi.org/10.1111/1467-9450.00237>

695 Cabeza, R., Albert, M., Belleville, S., Craik, F.I.M., Duarte, A., Grady, C.L., Lindenberger, U.,

696 Nyberg, L., Park, D.C., Reuter-Lorenz, P.A., Rugg, M.D., Steffener, J., Rajah, M.N., 2018.

697 Maintenance, reserve and compensation: the cognitive neuroscience of healthy ageing. *Nat. Rev.*

698 *Neurosci.* 19, 701–710. <https://doi.org/10.1038/s41583-018-0068-2>

699 Campbell, K.L., Grady, C.L., Ng, C., Hasher, L., 2012. Age differences in the frontoparietal cognitive

700 control network: Implications for distractibility. *Neuropsychologia* 50, 2212–2223.

701 <https://doi.org/10.1016/j.neuropsychologia.2012.05.025>

702 Carrier, J., Land, S., Buysse, D.J., Kupfer, D.J., Monk, T.H., 2001. The effects of age and gender on

703 sleep EEG power spectral density in the middle years of life (ages 20-60 years old).

704 *Psychophysiology* 38, 232–242. <https://doi.org/10.1017/S0048577201991838>

705 Chang, C., Cunningham, J.P., Glover, G.H., 2009. Influence of heart rate on the BOLD signal: The

706 cardiac response function. *Neuroimage* 44, 857–869.

707 <https://doi.org/10.1016/j.neuroimage.2008.09.029>

708 Chang, C., Leopold, D.A., Schölvinck, M.L., Mandelkow, H., Picchioni, D., Liu, X., Ye, F.Q., Turchi,

709 J.N., Duyn, J.H., 2016. Tracking brain arousal fluctuations with fMRI. *Proc. Natl. Acad. Sci.*

710 113, 4518–4523. <https://doi.org/10.1073/pnas.1520613113>

711 Chang, C., Liu, Z., Chen, M.C., Liu, X., Duyn, J.H., 2013. EEG correlates of time-varying BOLD

712 functional connectivity. *Neuroimage* 72, 227–236.

713 <https://doi.org/10.1016/j.neuroimage.2013.01.049>

714 Cho, Z., Chung, S., Lim, D., Wong, E.K., 1998. Effects of the Acoustic Noise of the Gradient Systems

715 on fMRI: *Magn. Reson. Med.* 39 331–335.

716 Cohen, M.X., 2017. Where Does EEG Come From and What Does It Mean? *Trends Neurosci.* 40,  
717 208–218. <https://doi.org/10.1016/j.tins.2017.02.004>

718 Cox, R.W., 1996. AFNI: Software for Analysis and Visualization of Functional Magnetic Resonance  
719 Neuroimages. *Comput. Biomed. Res.* 29, 162–173. <https://doi.org/10.1006/cbmr.1996.0014>

720 D’Esposito, M., Deouell, L.Y., Gazzaley, A., 2003. Alterations in the BOLD fMRI signal with ageing  
721 and disease: a challenge for neuroimaging. *Nat. Rev. Neurosci.* 4, 863–872.  
722 <https://doi.org/10.1038/nrn1246>

723 Damoiseaux, J.S., 2017. Effects of aging on functional and structural brain connectivity. *Neuroimage*  
724 160, 32–40. <https://doi.org/10.1016/j.neuroimage.2017.01.077>

725 Damoiseaux, J.S., Beckmann, C.F., Arigita, E.J.S., Barkhof, F., Scheltens, P., Stam, C.J., Smith, S.M.,  
726 Rombouts, S.A.R.B., 2008. Reduced resting-state brain activity in the “default network” in  
727 normal aging. *Cereb. Cortex* 18, 1856–1864. <https://doi.org/10.1093/cercor/bhm207>

728 Das, S.R., Pluta, J., Mancuso, L., Kliot, D., Yushkevich, P.A., Wolk, D.A., 2015. Anterior and  
729 posterior MTL networks in aging and MCI. *Neurobiol. Aging* 36, S141–S150.  
730 <https://doi.org/10.1016/j.neurobiolaging.2014.03.041>

731 Deligianni, F., Centeno, M., Carmichael, D.W., Clayden, J.D., 2014. Relating resting-state fMRI and  
732 EEG whole-brain connectomes across frequency bands. *Front. Neurosci.* 8, 1–16.  
733 <https://doi.org/10.3389/fnins.2014.00258>

734 Delorme, A., Makeig, S., 2004. EEGLAB: an open source toolbox for analysis of single-trail EEG  
735 dynamics including independent component analysis. *J. Neurosci. Methods* 134, 9–21.  
736 <https://doi.org/10.1016/j.jneumeth.2003.10.009>

737 Desikan, R.S., Ségonne, F., Fischl, B., Quinn, B.T., Dickerson, B.C., Blacker, D., Buckner, R.L.,  
738 Dale, A.M., Maguire, R.P., Hyman, B.T., Albert, M.S., Killiany, R.J., 2006. An automated  
739 labeling system for subdividing the human cerebral cortex on MRI scans into gyral based regions  
740 of interest. *Neuroimage* 31, 968–980. <https://doi.org/10.1016/j.neuroimage.2006.01.021>

741 Dierks, T., Jelic, V., Pascual-Marqui, R.D., Wahlund, L.O., Julin, P., Linden, D.E.J., Maurer, K.,  
742 Winblad, B., Nordberg, A., 2000. Spatial pattern of cerebral glucose metabolism (PET)  
743 correlates with localization of intracerebral EEG-generators in Alzheimer’s disease. *Clin.*  
744 *Neurophysiol.* 111, 1817–1824. [https://doi.org/10.1016/S1388-2457\(00\)00427-2](https://doi.org/10.1016/S1388-2457(00)00427-2)

745 Duffy, F.H., McAnulty, G.B., Albert, M.S., 1993. The pattern of age-related differences in  
746 electrophysiological activity of healthy males and females. *Neurobiol. Aging* 14, 73–84.  
747 [https://doi.org/10.1016/0197-4580\(93\)90025-7](https://doi.org/10.1016/0197-4580(93)90025-7)

748 Dustman, R.E., Shearer, D.E., Emmerson, R.Y., 1999. Life-span changes in EEG spectral amplitude,  
749 amplitude variability and mean frequency. *Clin. Neurophysiol.* 110, 1399–1409.  
750 [https://doi.org/10.1016/S1388-2457\(99\)00102-9](https://doi.org/10.1016/S1388-2457(99)00102-9)

751 Dustman, R.E., Shearer, D.E., Emmerson, R.Y., 1993. EEG and event-related potentials in normal

752 aging. *Prog. Neurobiol.* 41, 369–401. [https://doi.org/10.1016/0301-0082\(93\)90005-D](https://doi.org/10.1016/0301-0082(93)90005-D)

753 Engel, A.K., Fries, P., 2010. Beta-band oscillations-signalling the status quo? *Curr. Opin. Neurobiol.*  
754 20, 156–165. <https://doi.org/10.1016/j.conb.2010.02.015>

755 Failla, M., Grappiolo, A., Emanuelli, G., Vitale, G., Fraschini, N., Bigoni, M., Grieco, N., Denti, M.,  
756 Giannattasio, C., Mancia, G., 1999. Sympathetic tone restrains arterial distensibility of healthy  
757 and atherosclerotic subjects. *J. Hypertens.* 17, 1117–1123. <https://doi.org/10.1097/00004872-199917080-00011>

758 Farkas, E., Luiten, P.G.M., 2001. Cerebral microvascular pathology in aging and Alzheimer's disease,  
759 *Progress in Neurobiology*. [https://doi.org/10.1016/S0301-0082\(00\)00068-X](https://doi.org/10.1016/S0301-0082(00)00068-X)

760 Fernández, A., Zuluaga, P., Abásolo, D., Gómez, C., Serra, A., Méndez, M.A., Hornero, R., 2012.  
761 Brain oscillatory complexity across the life span. *Clin. Neurophysiol.* 123, 2154–2162.  
762 <https://doi.org/10.1016/j.clinph.2012.04.025>

763 Fischl, B., 2012. FreeSurfer. *Neuroimage* 62, 774–781.  
764 <https://doi.org/10.1016/j.neuroimage.2012.01.021>

765 Friston, K.J., Williams, S., Howard, R., Frackowiak, R.S.J., Turner, R., 1996. Movement-related  
766 effects in fMRI time-series. *Magn. Reson. Med.* 35, 346–355.  
767 <https://doi.org/10.1002/mrm.1910350312>

768 Garrett, D.D., Kovacevic, N., McIntosh, A.R., Grady, C.L., 2013a. The modulation of BOLD  
769 variability between cognitive states varies by age and processing speed. *Cereb. Cortex* 23, 684–  
770 693. <https://doi.org/10.1093/cercor/bhs055>

771 Garrett, D.D., Lindenberger, U., Hoge, R.D., Gauthier, C.J., 2017. Age differences in brain signal  
772 variability are robust to multiple vascular controls. *Sci. Rep.* 7, 10149.  
773 <https://doi.org/10.1038/s41598-017-09752-7>

774 Garrett, D.D., Nagel, I.E., Preuschhof, C., Burzynska, A.Z., Marchner, J., Wiegert, S., Jungehülsing,  
775 G.J., Nyberg, L., Villringer, A., Li, S.-C., Heekeren, H.R., Bäckman, L., Lindenberger, U., 2015.  
776 Amphetamine modulates brain signal variability and working memory in younger and older  
777 adults. *Proc. Natl. Acad. Sci.* 112, 7593–7598. <https://doi.org/10.1073/pnas.1504090112>

778 Garrett, D.D., Samanez-Larkin, G.R., MacDonald, S.W.S., Lindenberger, U., McIntosh, A.R., Grady,  
779 C.L., 2013b. Moment-to-moment brain signal variability: A next frontier in human brain  
780 mapping? *Neurosci. Biobehav. Rev.* 37, 610–624.  
781 <https://doi.org/10.1016/j.neubiorev.2013.02.015>

782 Geerligs, L., Tsvetanov, K.A., Cam-CAN, Henson, R.N., 2017. Challenges in measuring individual  
783 differences in functional connectivity using fMRI: The case of healthy aging. *Hum. Brain Mapp.*  
784 38, 4125–4156. <https://doi.org/10.1002/hbm.23653>

785 Golchert, J., Smallwood, J., Jefferies, E., Seli, P., Huntenburg, J.M., Liem, F., Lauckner, M.E.,  
786 Oligschläger, S., Bernhardt, B.C., Villringer, A., Margulies, D.S., 2017. Individual variation in  
787 intentionality in the mind-wandering state is reflected in the integration of the default-mode,  
788

789 fronto-parietal, and limbic networks. *Neuroimage* 146, 226–235.

790 <https://doi.org/10.1016/j.neuroimage.2016.11.025>

791 Goldman, R.I., Stern, J.M., Engel, J., Cohen, M.S., 2002. Simultaneous EEG and fMRI of the alpha

792 rhythm. *Neuroreport* 13, 2487–2492. <https://doi.org/10.1097/00001756-200212200-00022>

793 Gonçalves, S.I., De Munck, J.C., Pouwels, P.J.W., Schoonhoven, R., Kuijer, J.P.A., Maurits, N.M.,

794 Hoogduin, J.M., Van Someren, E.J.W., Heethaar, R.M., Lopes Da Silva, F.H., 2006. Correlating

795 the alpha rhythm to BOLD using simultaneous EEG/fMRI: Inter-subject variability. *Neuroimage*

796 30, 203–213. <https://doi.org/10.1016/j.neuroimage.2005.09.062>

797 Gong, G., He, Y., Evans, A.C., 2011. Brain connectivity: Gender makes a difference. *Neuroscientist*

798 17, 575–591. <https://doi.org/10.1177/1073858410386492>

799 Gorgolewski, K., Burns, C.D., Madison, C., Clark, D., Halchenko, Y.O., Waskom, M.L., Ghosh, S.S.,

800 2011. Nipype: A Flexible, Lightweight and Extensible Neuroimaging Data Processing

801 Framework in Python. *Front. Neuroinform.* 5, 13. <https://doi.org/10.3389/fninf.2011.00013>

802 Grady, C., 2012. The cognitive neuroscience of ageing. *Nat. Rev. Neurosci.* 13, 491–505.

803 <https://doi.org/10.1038/nrn3256>

804 Grady, C.L., Garrett, D.D., 2018. Brain signal variability is modulated as a function of internal and

805 external demand in younger and older adults. *Neuroimage* 169, 510–523.

806 <https://doi.org/10.1016/j.neuroimage.2017.12.031>

807 Grady, C.L., Garrett, D.D., 2014. Understanding variability in the BOLD signal and why it matters for

808 aging. *Brain Imaging Behav.* <https://doi.org/10.1007/s11682-013-9253-0>

809 Greicius, M.D., Srivastava, G., Reiss, A.L., Menon, V., 2004. Default-mode network activity

810 distinguishes Alzheimer's disease from healthy aging: evidence from functional MRI. *Proc. Natl.*

811 *Acad. Sci. U. S. A.* 101, 4637–42. <https://doi.org/10.1073/pnas.0308627101>

812 Gur, R.C., Gur, R.E., Obrist, W.D., Hungerbuhler, J.P., Younkin, D., Rosen, A.D., Skolnick, B.E.,

813 Reivich, M., 1982. Sex and handedness differences in cerebral blood flow during rest and

814 cognitive activity. *Science* (80-). 217, 659–661. <https://doi.org/10.1126/science.7089587>

815 Haimovici, A., Tagliazucchi, E., Balenzuela, P., Laufs, H., 2017. On wakefulness fluctuations as a

816 source of BOLD functional connectivity dynamics. *Sci. Rep.* 7. <https://doi.org/10.1038/s41598-017-06389-4>

817 Hartikainen, P., Soininen, H., Partanen, J., Helkala, E.L., Riekkinen, P., 1992. Aging and spectral

818 analysis of EEG in normal subjects: a link to memory and CSF AChE. *Acta Neurol. Scand.* 86,

819 148–155. <https://doi.org/10.1111/j.1600-0404.1992.tb05057.x>

820 Haufe, S., Ewald, A., 2016. A Simulation Framework for Benchmarking EEG-Based Brain

821 Connectivity Estimation Methodologies. *Brain Topogr.* 1–18. <https://doi.org/10.1007/s10548-016-0498-y>

822 Hawkes, C.H., Prescott, R.J., 1973. EEG variation in healthy subjects. *Electroencephalogr. Clin.*

823 *Neurophysiol.* 34, 197–199. [https://doi.org/10.1016/0013-4694\(73\)90048-5](https://doi.org/10.1016/0013-4694(73)90048-5)

826 Huang, Y., Parra, L.C., Haufe, S., 2016. The New York Head—A precise standardized volume  
827 conductor model for EEG source localization and tES targeting. *Neuroimage* 140, 150–162.  
828 <https://doi.org/10.1016/j.neuroimage.2015.12.019>

829 Hudetz, A.G., Biswal, B.B., Shen, H., Lauer, K.K., Kampine, J.P., 1998. Spontaneous Fluctuations in  
830 Cerebral Oxygen Supply. Springer, Boston, MA, pp. 551–559. [https://doi.org/10.1007/978-1-4615-4863-8\\_66](https://doi.org/10.1007/978-1-4615-4863-8_66)

832 Immer, F.R., 1937. Correlation between Means and Standard Deviations in Field Experiments. *J. Am.  
833 Stat. Assoc.* 32, 525–531. <https://doi.org/10.1080/01621459.1937.10502321>

834 Jacobson, S.C., Blanchard, M., Connolly, C.C., Cannon, M., Garavan, H., 2011. An fMRI  
835 investigation of a novel analogue to the Trail-Making Test. *Brain Cogn.* 77, 60–70.  
836 <https://doi.org/10.1016/j.bandc.2011.06.001>

837 Jaušovec, N., Jaušovec, K., 2010. Resting brain activity: Differences between genders.  
838 *Neuropsychologia* 48, 3918–3925. <https://doi.org/10.1016/j.neuropsychologia.2010.09.020>

839 Jenkinson, M., Beckmann, C.F., Behrens, T.E.J., Woolrich, M.W., Smith, S.M., 2012. Fsl.  
840 *Neuroimage* 62, 782–790. <https://doi.org/10.1016/j.neuroimage.2011.09.015>

841 Jolliffe, I.T., Cadima, J., 2016. Principal component analysis: A review and recent developments.  
842 *Philos. Trans. R. Soc. A Math. Phys. Eng. Sci.* 374, 20150202.  
843 <https://doi.org/10.1098/rsta.2015.0202>

844 Jorge, J., Van der Zwaag, W., Figueiredo, P., 2014. EEG-fMRI integration for the study of human  
845 brain function. *Neuroimage* 102, 24–34. <https://doi.org/10.1016/j.neuroimage.2013.05.114>

846 Jurcak, V., Tsuzuki, D., Dan, I., 2007. 10/20, 10/10, and 10/5 systems revisited: Their validity as  
847 relative head-surface-based positioning systems. *Neuroimage* 34, 1600–1611.  
848 <https://doi.org/10.1016/j.neuroimage.2006.09.024>

849 Kielar, A., Deschamps, T., Chu, R.K.O., Jokel, R., Khatamian, Y.B., Chen, J.J., Meltzer, J.A., 2016.  
850 Identifying dysfunctional cortex: Dissociable effects of stroke and aging on resting state  
851 dynamics in MEG and fmri. *Front. Aging Neurosci.* 8. <https://doi.org/10.3389/fnagi.2016.00040>

852 Klimesch, W., 1999. EEG alpha and theta oscillations reflect cognitive and memory performance: A  
853 review and analysis. *Brain Res. Rev.* 29, 169–195. [https://doi.org/10.1016/S0165-0173\(98\)00056-3](https://doi.org/10.1016/S0165-0173(98)00056-3)

855 Labrenz, F., Ferri, F., Wrede, K., Forsting, M., Schedlowski, M., Engler, H., Elsenbruch, S., Benson,  
856 S., Costantini, M., 2018. Altered temporal variance and functional connectivity of BOLD signal  
857 is associated with state anxiety during acute systemic inflammation. *Neuroimage* 184, 916–924.  
858 <https://doi.org/10.1016/j.neuroimage.2018.09.056>

859 Latta, F., Leproult, R., Tasali, E., Hofmann, E., Van Cauter, E., 2005. Sex differences in delta and  
860 alpha EEG activities in healthy older adults. *Sleep* 28, 1525–1534.  
861 <https://doi.org/10.1093/sleep/28.12.1525>

862 Laufs, H., Kleinschmidt, A., Holt, J.L., Elfont, R., Krams, M., Paul, J.S., Krakow, K., 2006. Where the

863 BOLD signal goes when alpha EEG leaves. *Neuroimage* 31, 1408–1418.

864 <https://doi.org/10.1016/j.neuroimage.2006.02.002>

865 Laufs, H., Krakow, K., Sterzer, P., Eger, E., Beyerle, A., Kleinschmidt, A., 2003.

866 Electroencephalographic signatures of attentional and cognitive default modes in spontaneous

867 brain activity fluctuations at rest 100.

868 Lipsitz, L.A., Goldberger, A.L., 1992. Loss of ‘Complexity’ and Aging: Potential Applications of

869 Fractals and Chaos Theory to Senescence. *JAMA J. Am. Med. Assoc.* 267, 1806–1809.

870 <https://doi.org/10.1001/jama.1992.03480130122036>

871 Liu, P., Hebrank, A.C., Rodrigue, K.M., Kennedy, K.M., Section, J., Park, D.C., Lu, H., 2013. Age-

872 related differences in memory-encoding fMRI responses after accounting for decline in vascular

873 reactivity. *Neuroimage* 78, 415–425. <https://doi.org/10.1016/j.neuroimage.2013.04.053>

874 Liu, T.T., 2013. Neurovascular factors in resting-state functional MRI. *Neuroimage* 80, 339–348.

875 <https://doi.org/10.1016/j.neuroimage.2013.04.071>

876 Logothetis, N.K., 2008. What we can do and what we cannot do with fMRI. *Nature* 453, 869–878.

877 <https://doi.org/10.1038/nature06976>

878 Logothetis, N.K., Wandell, B.A., 2004. Interpreting the BOLD Signal. *Annu. Rev. Physiol.* 66, 735–

879 769. <https://doi.org/10.1146/annurev.physiol.66.082602.092845>

880 Lopes Da Silva, F.H., Pijn, J.P., Velis, D., Nijssen, P.C.G., 1997. Alpha rhythms: Noise, dynamics and

881 models. *Int. J. Psychophysiol.* 26, 237–249. [https://doi.org/10.1016/S0167-8760\(97\)00767-8](https://doi.org/10.1016/S0167-8760(97)00767-8)

882 Lopez-Larson, M.P., Anderson, J.S., Ferguson, M.A., Yurgelun-Todd, D., 2011. Local brain

883 connectivity and associations with gender and age. *Dev. Cogn. Neurosci.* 1, 187–197.

884 <https://doi.org/10.1016/j.dcn.2010.10.001>

885 Ma, Y., Shaik, M.A., Kozberg, M.G., Kim, S.H., Portes, J.P., Timerman, D., Hillman, E.M.C., 2016.

886 Resting-state hemodynamics are spatiotemporally coupled to synchronized and symmetric neural

887 activity in excitatory neurons. *Proc. Natl. Acad. Sci.* 113, E8463–E8471.

888 <https://doi.org/10.1073/pnas.1525369113>

889 Malone, I.B., Leung, K.K., Clegg, S., Barnes, J., Whitwell, J.L., Ashburner, J., Fox, N.C., Ridgway,

890 G.R., 2015. Accurate automatic estimation of total intracranial volume: A nuisance variable with

891 less nuisance. *Neuroimage* 104, 366–372. <https://doi.org/10.1016/j.neuroimage.2014.09.034>

892 Maltez, J., Hyllienmark, L., Nikulin, V. V., Brismar, T., 2004. Time course and variability of power in

893 different frequency bands of EEG during resting conditions. *Neurophysiol. Clin.* 34, 195–202.

894 <https://doi.org/10.1016/j.neucli.2004.09.003>

895 Mantini, D., Perrucci, M.G., Del Gratta, C., Romani, G.L., Corbetta, M., 2007. Electrophysiological

896 signatures of resting state networks in the human brain. *Proc. Natl. Acad. Sci.* 104, 13170–

897 13175. <https://doi.org/10.1073/pnas.0700668104>

898 Margulies, D.S., Ghosh, S.S., Goulas, A., Falkiewicz, M., Huntenburg, J.M., Langs, G., Bezgin, G.,

899 Eickhoff, S.B., Castellanos, F.X., Petrides, M., Jefferies, E., Smallwood, J., 2016. Situating the

900 default-mode network along a principal gradient of macroscale cortical organization. *Proc. Natl.*  
901 *Acad. Sci.* 113, 12574–12579. <https://doi.org/10.1073/pnas.1608282113>

902 Martin, J., Friston, K.J., Colebatch, J.G., Frackowiak, R.S.J., Unit, M.R.C.C., Hospital, H., 1991.  
903 Decreases in Regional Cerebral Blood Flow with Normal Aging 684–689.

904 Mateo, C., Knutson, P.M., Tsai, P.S., Shih, A.Y., Kleinfeld, D., 2017. Entrainment of Arteriole  
905 Vasomotor Fluctuations by Neural Activity Is a Basis of Blood-Oxygenation-Level-Dependent  
906 “Resting-State” Connectivity. *Neuron* 96, 936-948.e3.  
907 <https://doi.org/10.1016/j.neuron.2017.10.012>

908 Matsuura, M., Yamamoto, K., Fukuzawa, H., Okubo, Y., Uesugi, H., Moriwa, M., Kojima, T.,  
909 Shimazono, Y., 1985. Age development and sex differences of various EEG elements in healthy  
910 children and adults - Quantification by a computerized waveform recognition method.  
911 *Electroencephalogr. Clin. Neurophysiol.* 60, 394–406. [https://doi.org/10.1016/0013-4694\(85\)91013-2](https://doi.org/10.1016/0013-4694(85)91013-2)

912 McBride, J.C., Zhao, X., Munro, N.B., Smith, C.D., Jicha, G.A., Hively, L., Broster, L.S., Schmitt,  
913 F.A., Kryscio, R.J., Jiang, Y., 2014. Spectral and complexity analysis of scalp EEG  
914 characteristics for mild cognitive impairment and early Alzheimer’s disease. *Comput. Methods  
915 Programs Biomed.* 114, 153–163. <https://doi.org/10.1016/j.cmpb.2014.01.019>

916 McDonald, J.H., 2014. *Handbook of Biological Statistics*. Sparky House Publ. 180–185.

917 Meunier, D., Achard, S., Morcom, A., Bullmore, E., 2009. Age-related changes in modular  
918 organization of human brain functional networks. *Neuroimage* 44, 715–723.  
919 <https://doi.org/10.1016/j.neuroimage.2008.09.062>

920 Meyer, M.C., Janssen, R.J., Van Oort, E.S.B., Beckmann, C.F., Barth, M., 2013. The Quest for EEG  
921 Power Band Correlation with ICA Derived fMRI Resting State Networks. *Front. Hum. Neurosci.*  
922 7, 315. <https://doi.org/10.3389/fnhum.2013.00315>

923 Moosmann, M., Ritter, P., Krastel, I., Brink, A., Thees, S., Blankenburg, F., Taskin, B., Obrig, H.,  
924 Villringer, A., 2003. Correlates of alpha rhythm in functional magnetic resonance imaging and  
925 near infrared spectroscopy. *Neuroimage* 20, 145–158. [https://doi.org/10.1016/S1053-8119\(03\)00344-6](https://doi.org/10.1016/S1053-8119(03)00344-6)

926 Moretti, D. V., Paternicò, D., Binetti, G., Zanetti, O., Frisoni, G.B., 2012. EEG markers are associated  
927 to gray matter changes in thalamus and basal ganglia in subjects with mild cognitive impairment.  
928 *Neuroimage* 60, 489–496. <https://doi.org/10.1016/j.neuroimage.2011.11.086>

929 Murayama, Y., Bießmann, F., Logothetis, N.K., Oeltermann, A., Müller, K.-R., Meinecke, F.C.,  
930 Augath, M., 2010. Relationship between neural and hemodynamic signals during spontaneous  
931 activity studied with temporal kernel CCA. *Magn. Reson. Imaging* 28, 1095–1103.  
932 <https://doi.org/10.1016/j.mri.2009.12.016>

933 Murphy, K., Birn, R.M., Bandettini, P.A., 2013. Resting-state fMRI confounds and cleanup.  
934 *Neuroimage* 80, 349–359. <https://doi.org/10.1016/j.neuroimage.2013.04.001>

937 Näpflin, M., Wildi, M., Sarnthein, J., 2007. Test-retest reliability of resting EEG spectra validates a  
938 statistical signature of persons. *Clin. Neurophysiol.* 118, 2519–2524.  
939 <https://doi.org/10.1016/j.clinph.2007.07.022>

940 Nguyen, L.H., Holmes, S., 2019. Ten quick tips for effective dimensionality reduction. *PLOS Comput.*  
941 *Biol.* 15, e1006907. <https://doi.org/10.1371/journal.pcbi.1006907>

942 Niessing, J., Ebisch, B., Schmidt, K.E., Niessing, M., Singer, W., Galuske, R.A.W., 2005.  
943 Neuroscience: Hemodynamic signals correlate tightly with synchronized gamma oscillations.  
944 *Science* (80-. ). 309, 948–951. <https://doi.org/10.1126/science.1110948>

945 Nir, Y., Hasson, U., Levy, I., Yeshurun, Y., Malach, R., 2006. Widespread functional connectivity and  
946 fMRI fluctuations in human visual cortex in the absence of visual stimulation. *Neuroimage* 30,  
947 1313–1324. <https://doi.org/10.1016/j.neuroimage.2005.11.018>

948 Nomi, J.S., Bolt, T.S., Ezie, C.E.C., Uddin, L.Q., Heller, A.S., 2017. Moment-to-Moment BOLD  
949 Signal Variability Reflects Regional Changes in Neural Flexibility across the Lifespan. *J.*  
950 *Neurosci.* 37, 5539–5548. <https://doi.org/10.1523/JNEUROSCI.3408-16.2017>

951 Nomi, J.S., Schettini, E., Voorhies, W., Bolt, T.S., Heller, A.S., Uddin, L.Q., 2018. Resting-State  
952 Brain Signal Variability in Prefrontal Cortex Is Associated With ADHD Symptom Severity in  
953 Children. *Front. Hum. Neurosci.* 12, 90. <https://doi.org/10.3389/fnhum.2018.00090>

954 Nunez, P.L., Srinivasan, R., Fields, R.D., 2015. EEG functional connectivity, axon delays and white  
955 matter disease. *Clin. Neurophysiol.* 126, 110–120. <https://doi.org/10.1016/j.clinph.2014.04.003>

956 Oken, B.S., Chiappa, K.H., 1988. Short-term variability in EEG frequency analysis.  
957 *Electroencephalogr. Clin. Neurophysiol.* 69, 191–198. [https://doi.org/10.1016/0013-4694\(88\)90128-9](https://doi.org/10.1016/0013-4694(88)90128-9)

959 Petersen, S.E., Savalia, N.K., Chan, M.Y., Park, D.C., Wig, G.S., 2014. Decreased segregation of  
960 brain systems across the healthy adult lifespan. *Proc. Natl. Acad. Sci.* 111, E4997–E5006.  
961 <https://doi.org/10.1073/pnas.1415122111>

962 Qin, Y., Jiang, S., Zhang, Q., Dong, L., Jia, X., He, H., Yao, Y., Yang, H., Zhang, T., Luo, C., Yao,  
963 D., 2019. BOLD-fMRI activity informed by network variation of scalp EEG in juvenile  
964 myoclonic epilepsy. *NeuroImage Clin.* 22, 101759. <https://doi.org/10.1016/j.nicl.2019.101759>

965 Quandt, F., Bönstrup, M., Schulz, R., Timmermann, J.E., Zimmerman, M., Nolte, G., Hummel, F.C.,  
966 2016. Spectral variability in the aged brain during fine motor control. *Front. Aging Neurosci.* 8.  
967 <https://doi.org/10.3389/fnagi.2016.00305>

968 Raichle, M.E., 2015. The Brain's Default Mode Network. *Annu. Rev. Neurosci.* 38, 433–447.  
969 <https://doi.org/10.1146/annurev-neuro-071013-014030>

970 Reitan, R.M., 1955. Certain differential effects of left and right cerebral lesions in human adults. *J*  
971 *Comp Physiol Psychol* 48, 474–477.

972 Reitan, R.M., Wolfson, D., 1995. Category Test and Trail Making Test as Measures of Frontal Lobe  
973 Functions. *Clin. Neuropsychol.* 9, 50–56. <https://doi.org/10.1080/13854049508402057>

974 Rice, J.K., Rorden, C., Little, J.S., Parra, L.C., 2013. Subject position affects EEG magnitudes.  
975 *Neuroimage* 64, 476–484. <https://doi.org/10.1016/j.neuroimage.2012.09.041>

976 Ritter, P., Moosmann, M., Villringer, A., 2009. Rolandic alpha and beta EEG rhythms' strengths are  
977 inversely related to fMRI-BOLD signal in primary somatosensory and motor cortex. *Hum. Brain*  
978 *Mapp.* 30, 1168–1187. <https://doi.org/10.1002/hbm.20585>

979 Ritter, P., Villringer, A., 2006. Simultaneous EEG-fMRI. *Neurosci. Biobehav. Rev.* 30, 823–838.  
980 <https://doi.org/10.1016/j.neubiorev.2006.06.008>

981 Rodriguez, G., Warkentin, S., Risberg, J., Rosadini, G., 1988. Sex differences in regional cerebral  
982 blood flow. *J. Cereb. Blood Flow Metab.* 8, 783–789. <https://doi.org/10.1038/jcbfm.1988.133>

983 Rokem, a, Trumppis, M., Perez, F., 2009. Nitime: time-series analysis for neuroimaging data. *Proc. 8th*  
984 *Python Sci. Conf. (SciPy 2009)* 1–8.

985 Rosenblum, M., Pikovsky, A., Kurths, J., Schäfer, C., Tass, P.A., 2001. Phase synchronization: From  
986 theory to data analysis. *Handb. Biol. Phys.* 4, 279–321. [https://doi.org/10.1016/S1383-8121\(01\)80012-9](https://doi.org/10.1016/S1383-8121(01)80012-9)

988 Rossiter, H.E., Davis, E.M., Clark, E. V., Boudrias, M.H., Ward, N.S., 2014. Beta oscillations reflect  
989 changes in motor cortex inhibition in healthy ageing. *Neuroimage* 91, 360–365.  
990 <https://doi.org/10.1016/j.neuroimage.2014.01.012>

991 Ruigrok, A.N.V., Salimi-Khorshidi, G., Lai, M.C., Baron-Cohen, S., Lombardo, M. V., Tait, R.J.,  
992 Suckling, J., 2014. A meta-analysis of sex differences in human brain structure. *Neurosci.*  
993 *Biobehav. Rev.* 39, 34–50. <https://doi.org/10.1016/j.neubiorev.2013.12.004>

994 Sacher, J., Neumann, J., Okon-Singer, H., Gotowiec, S., Villringer, A., 2013. Sexual dimorphism in  
995 the human brain: Evidence from neuroimaging. *Magn. Reson. Imaging* 31, 366–375.  
996 <https://doi.org/10.1016/j.mri.2012.06.007>

997 Scheeringa, R., Fries, P., Petersson, K.M., Oostenveld, R., Grothe, I., Norris, D.G., Hagoort, P.,  
998 Bastiaansen, M.C.M., 2011. Neuronal Dynamics Underlying High- and Low-Frequency EEG  
999 Oscillations Contribute Independently to the Human BOLD Signal. *Neuron* 69, 572–583.  
1000 <https://doi.org/10.1016/j.neuron.2010.11.044>

1001 Seaquist, E.R., Chen, W., Benedict, L.E., Ugurbil, K., Kwag, J.H., Zhu, X.H., Nelson, C.A., 2007.  
1002 Insulin reduces the BOLD response but is without effect on the VEP during presentation of a  
1003 visual task in humans. *J. Cereb. Blood Flow Metab.* 27, 154–160.  
1004 <https://doi.org/10.1038/sj.jcbfm.9600316>

1005 Shehzad, Z., Kelly, A.M.C., Reiss, P.T., Gee, D.G., Gotimer, K., Uddin, L.Q., Lee, S.H., Margulies,  
1006 D.S., Roy, A.K., Biswal, B.B., Petkova, E., Castellanos, F.X., Milham, M.P., 2009. The Resting  
1007 Brain: Unconstrained yet Reliable. *Cereb. Cortex* 19, 2209–2229.  
1008 <https://doi.org/10.1093/cercor/bhn256>

1009 Sleimen-Malkoun, R., Perdikis, D., Muller, V., Blanc, J.-L., Huys, R., Temprado, J.-J., Jirsa, V.K.,  
1010 2015. Brain Dynamics of Aging: Multiscale Variability of EEG Signals at Rest and during an

1011        Auditory Oddball Task. *eNeuro* 2. <https://doi.org/10.1523/ENEURO.0067-14.2015>

1012        Smits, F.M., Porcaro, C., Cottone, C., Cancelli, A., Rossini, P.M., Tecchio, F., 2016.

1013        Electroencephalographic fractal dimension in healthy ageing and Alzheimer's disease. *PLoS One*  
1014        11, 1–16. <https://doi.org/10.1371/journal.pone.0149587>

1015        Speelman, C.P., McGann, M., 2013. How mean is the mean? *Front. Psychol.* 4, 1–12.  
1016        <https://doi.org/10.3389/fpsyg.2013.00451>

1017        Spreng, R.N., Sepulcre, J., Turner, G.R., Stevens, W.D., Schacter, D.L., 2013. Intrinsic Architecture  
1018        Underlying the Relations among the Default, Dorsal Attention, and Frontoparietal Control  
1019        Networks of the Human Brain. *J. Cogn. Neurosci.* 25, 74–86.  
1020        [https://doi.org/10.1162/jocn\\_a\\_00281](https://doi.org/10.1162/jocn_a_00281)

1021        Steriade, M., 2006. Grouping of brain rhythms in corticothalamic systems. *Neuroscience* 137, 1087–  
1022        1106. <https://doi.org/10.1016/j.neuroscience.2005.10.029>

1023        Stomrud, E., Hansson, O., Minthon, L., Blennow, K., Rosén, I., Londos, E., 2010. Slowing of EEG  
1024        correlates with CSF biomarkers and reduced cognitive speed in elderly with normal cognition  
1025        over 4 years. *Neurobiol. Aging* 31, 215–223.  
1026        <https://doi.org/10.1016/j.neurobiolaging.2008.03.025>

1027        Tagliazucchi, E., Laufs, H., 2014. Decoding Wakefulness Levels from Typical fMRI Resting-State  
1028        Data Reveals Reliable Drifts between Wakefulness and Sleep. *Neuron* 82, 695–708.  
1029        <https://doi.org/10.1016/j.neuron.2014.03.020>

1030        Thompson, G.J., 2018. Neural and metabolic basis of dynamic resting state fMRI. *Neuroimage* 180,  
1031        448–462. <https://doi.org/10.1016/j.neuroimage.2017.09.010>

1032        Tibshirani, R., 2011. Regression shrinkage and selection via the lasso: a retrospective. *J. R. Stat. Soc.*  
1033        Ser. B (Statistical Methodol.

1034        73, 273–282. <https://doi.org/10.1111/j.1467-9868.2011.00771.x>

1035        Tomasi, D., Volkow, N.D., 2012. Aging and functional brain networks. *Mol. Psychiatry* 17, 549–558.  
1036        <https://doi.org/10.1038/mp.2011.81>

1037        Tsvetanov, K.A., Henson, R.N.A., Tyler, L.K., Davis, S.W., Shafto, M.A., Taylor, J.R., Williams, N.,  
1038        Cam-Can, Rowe, J.B., 2015. The effect of ageing on fMRI: Correction for the confounding  
1039        effects of vascular reactivity evaluated by joint fMRI and MEG in 335 adults. *Hum. Brain Mapp.*  
1040        36, 2248–2269. <https://doi.org/10.1002/hbm.22768>

1041        Vaillancourt, D.E., Newell, K.M., 2002. Changing complexity in human behavior and physiology  
1042        through aging and disease. *Neurobiol Aging* 23, 1–11. [https://doi.org/10.1016/S0197-4580\(02\)00052-0](https://doi.org/10.1016/S0197-4580(02)00052-0)

1043        Valdés-Hernández, P.A., Ojeda-González, A., Martínez-Montes, E., Lage-Castellanos, A., Virués-  
1044        Alba, T., Valdés-Urrutia, L., Valdes-Sosa, P.A., 2010. White matter architecture rather than  
1045        cortical surface area correlates with the EEG alpha rhythm. *Neuroimage* 49, 2328–2339.  
1046        <https://doi.org/10.1016/j.neuroimage.2009.10.030>

1047        Veldhuizen, R.J., Jonkman, E.J., Poortvliet, D.C.J., 1993. Sex differences in age regression parameters

1048 of healthy adults—normative data and practical implications. *Electroencephalogr. Clin.*  
1049 *Neurophysiol.* 86, 377–384. [https://doi.org/10.1016/0013-4694\(93\)90133-G](https://doi.org/10.1016/0013-4694(93)90133-G)

1050 Villringer, A., Dirnagl, U., 1995. Coupling of brain activity and cerebral blood flow: basis of  
1051 functional neuroimaging. *Cerebrovasc. Brain Metab. Rev.* 7, 240—276.

1052 Vlahou, E.L., Thurm, F., Kolassa, I.-T., Schlee, W., 2015. Resting-state slow wave power, healthy  
1053 aging and cognitive performance. *Sci. Rep.* 4, 5101. <https://doi.org/10.1038/srep05101>

1054 Wang, R., Foniok, T., Wamsteeker, J.I., Qiao, M., Tomanek, B., Vivanco, R.A., Tuor, U.I., 2006.  
1055 Transient blood pressure changes affect the functional magnetic resonance imaging detection of  
1056 cerebral activation. *Neuroimage* 31, 1–11. <https://doi.org/10.1016/j.neuroimage.2005.12.004>

1057 Wheeler, R.E., 2016. lmPerm: Permutation tests for linear models. <http://CRAN.R-project.org/package=lmPerm>. 24 p.

1059 Witten, D.M., Tibshirani, R., Hastie, T., 2009. A penalized matrix decomposition, with applications to  
1060 sparse principal components and canonical correlation analysis. *Biostatistics* 10, 515–534.  
1061 <https://doi.org/10.1093/biostatistics/kxp008>

1062 Wong, C.W., Olafsson, V., Tal, O., Liu, T.T., 2013. The amplitude of the resting-state fMRI global  
1063 signal is related to EEG vigilance measures. *Neuroimage* 83, 983–990.  
1064 <https://doi.org/10.1016/j.neuroimage.2013.07.057>

1065 Yan, C.G., Craddock, R.C., Zuo, X.N., Zang, Y.F., Milham, M.P., 2013. Standardizing the intrinsic  
1066 brain: Towards robust measurement of inter-individual variation in 1000 functional  
1067 connectomes. *Neuroimage* 80, 246–262. <https://doi.org/10.1016/j.neuroimage.2013.04.081>

1068 Yang, A.C., Huang, C.C., Yeh, H.L., Liu, M.E., Hong, C.J., Tu, P.C., Chen, J.F., Huang, N.E., Peng,  
1069 C.K., Lin, C.P., Tsai, S.J., 2013. Complexity of spontaneous BOLD activity in default mode  
1070 network is correlated with cognitive function in normal male elderly: A multiscale entropy  
1071 analysis. *Neurobiol. Aging* 34, 428–438. <https://doi.org/10.1016/j.neurobiolaging.2012.05.004>

1072 Yu, Q., Wu, L., Bridwell, D.A., Erhardt, E.B., Du, Y., He, H., Chen, J., Liu, P., Sui, J., Pearlson, G.,  
1073 Calhoun, V.D., 2016. Building an EEG-fMRI Multi-Modal Brain Graph: A Concurrent EEG-  
1074 fMRI Study. *Front. Hum. Neurosci.* 10, 1–17. <https://doi.org/10.3389/fnhum.2016.00476>

1075 Zakzanis, K., Mraz, R., Graham, S., 2005. An fMRI study of the trail making test. *Neuropsychologia*.

1076 Zappasodi, F., Marzetti, L., Olejarczyk, E., Tecchio, F., Pizzella, V., 2015. Age-related changes in  
1077 electroencephalographic signal complexity. *PLoS One* 10, 1–13.  
1078 <https://doi.org/10.1371/journal.pone.0141995>

1079 Zappasodi, F., Pasqualetti, P., Tombini, M., Ercolani, M., Pizzella, V., Rossini, P.M., Tecchio, F.,  
1080 2006. Hand cortical representation at rest and during activation: Gender and age effects in the  
1081 two hemispheres. *Clin. Neurophysiol.* 117, 1518–1528.  
1082 <https://doi.org/10.1016/j.clinph.2006.03.016>

1083 Ziegler, E., Chellappa, S.L., Gaggioni, G., Ly, J.Q.M., Vandewalle, G., André, E., Geuzaine, C.,  
1084 Phillips, C., 2014. A finite-element reciprocity solution for EEG forward modeling with realistic

1085 individual head models. *Neuroimage* 103, 542–551.

1086 <https://doi.org/10.1016/j.neuroimage.2014.08.056>

1087 Zöller, D., Schaer, M., Scariati, E., Padula, M.C., Eliez, S., Van De Ville, D., 2017. Disentangling  
1088 resting-state BOLD variability and PCC functional connectivity in 22q11.2 deletion syndrome.

1089 *Neuroimage* 149, 85–97. <https://doi.org/10.1016/j.neuroimage.2017.01.064>

1090 Zuo, X.N., Di Martino, A., Kelly, C., Shehzad, Z.E., Gee, D.G., Klein, D.F., Castellanos, F.X.,  
1091 Biswal, B.B., Milham, M.P., 2010. The oscillating brain: Complex and reliable. *Neuroimage* 49,  
1092 1432–1445. <https://doi.org/10.1016/j.neuroimage.2009.09.037>

1093